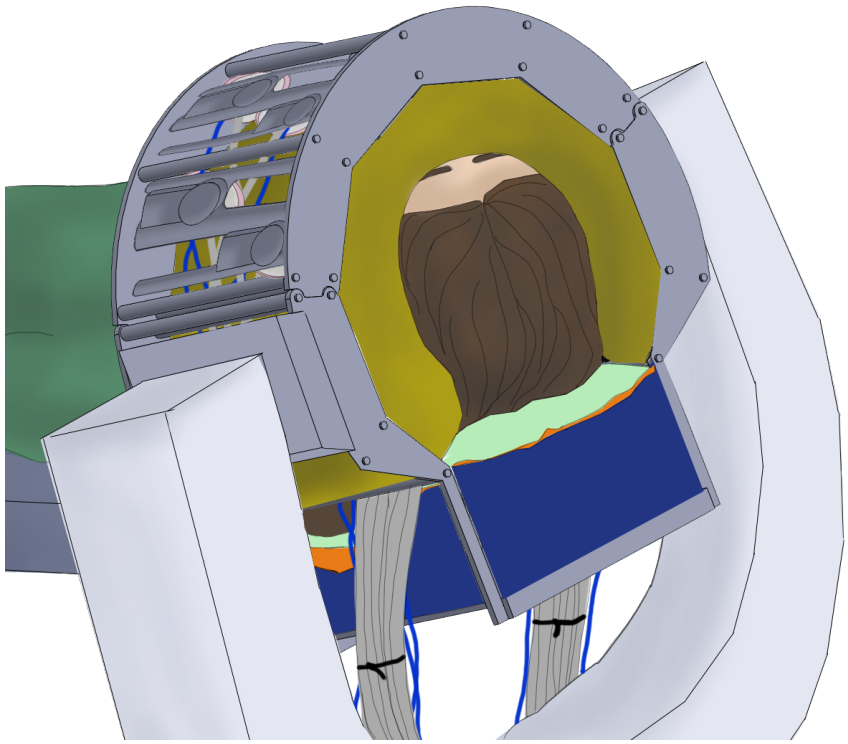

Design of Head Applicator for Hyperthermia Treatment

Bringing hyperthermia closer to clinical use

Master's Thesis in Biomedical Engineering

Andrea Nygren
nygrena@student.chalmers.se

Department of Electrical Engineering
Chalmers University of Technology
Göteborg, Sweden
January, 2020

Supervisor: Assistant Professor Hana Dobšíček Trefnà, Department of Electrical Engingeering
Examiner: Associate Professor Andreas Fhager, Department of Electrical Engineering

Cover: A sketch of the head applicator designed during the project.
All figures/photos in the report without a reference are drawn/taken by the author.

Typeset in LaTeX

Design of Head Applicator for Hyperthermia Treatment
Bringing hyperthermia closer to clinical use
ANDREA NYGREN

Department of Electrical Engineering
Chalmers University of Technology
SE-412 96 Göteborg, Sweden
Telephone +46 31 772 1000

Design of Head Applicator for Hyperthermia Treatment

Bringing hyperthermia closer to clinical use

Andrea Nygren
Department of Electrical Engineering
Chalmers University of Technology

Abstract

Head and neck cancer is the sixth leading cause of cancer-related death worldwide. The survival and relapse rates for this disease are somber, indicating a need to improve the current treatment methods. Studies have shown that combining radio- and chemotherapy with hyperthermia significantly increases treatment outcome. The project aims to develop a head applicator for hyperthermia treatment, including design of a water bolus. The standard solution of a water-filled plastic bag was compared to a novel hydrogel-based bolus. The cooling ability of the boli was evaluated experimentally through studying the temperature change over time with and without an external heat source (a microwave antenna). The boli and material types for the waterbag were evaluated using Kesselring matrices. The results indicate that a waterbag-type bolus is the most efficient. The material determined most appropriate was latex spray. Due to the complex geometry of the head, two boli should be used simultaneously: one smaller around the neck and a wider one covering the neck bolus and the head of the patient. The applicator will have two rings of 8 antennas, working at frequencies from 430-900 MHz. The antenna positions can be adjusted using motors and the exact position of the applicator can be set using a positioning machine. Patient movement is minimised during treatment using a vacuum bag. The head applicator frame is made of two large plastic plates, held together by 3D printed pins and screws. The back of the neck has no antennas, making room for a head support and for antenna wires and cooling tubes to exit the applicator. The proposed head applicator requires more work before implementation but is a good starting point for what in the close future can be brought to clinical use.

Keywords: Hyperthermia, H&N, Applicator, Bolus, Treatment, Tumour, Cancer, Microwaves

Acknowledgements

First of all, I would like to thank my supervisor Hana Dobšíček Trefná for her support and the opportunity to, once again, take part in a very interesting project. It has been fascinating to work on so many different projects within hyperthermia research and I will bring many lessons with me in my future work.

A big thank you to Massimiliano Zanoli for your help with the experiments and taking the time to discuss with me. Vase Petrov, thank you and thank you again for not just introducing me to the lab but for solving every problem I came to you with. To everyone who I have interacted with in the lab this semester, your company has always brightened up my days and I have really appreciated it.

I want to thank Håkan Torén for taking the time to help me, and all the amazing things you construct for the lab. Thank you to Saül Llacer Navarro for introducing me to the programs and your help in the start. Finally, I would like to thank Andreas Fhager for agreeing to be my examiner.

Andrea Nygren, Göteborg, January 15, 2020

Contents

List of Abbreviations

CSF	Cerebrospinal Fluid
CT	Chemotherapy (Note, once used to refer to Computer Tomography, in figure 2)
EM	Electromagnetism
FCC	Federal Communications Commission
H&N	Head and Neck
HNSCC	Head and Neck Squamous Cell Carcinomas
HTP	Hyperthermia Treatment Planning
LBG	Locust Bean Gum
LQ	Linear-Quadratic
MRI	Magnetic Resonance Imaging
MW	Microwave
PTS	Post- och Telestyrelsen
RF	Radio Frequency
RT	Radiotherapy
SF	Surviving Fraction
UWB	Ultra Wide Band
WB	Water Bolus

List of Figures

List of Tables

1 Introduction

Head and neck (H&N) cancer is the sixth leading cause of cancer-related death worldwide [6]. It includes cancers originating in the nasal cavity, sinuses, lips, mouth, salviary glands, throat and larynx. These tumours arise in the epithelial cells lining the mucosal surfaces of the head and neck, and are called squamous cell carcinomas (HNSCC) [7]. When caught in the early stages of the disease, the cure rate is high when using single-modality treatments such as surgery or radiation therapy (RT) [8]. In later stages when the disease has progressed to locally advanced, these types of HNSCC are usually treated with multi-modality treatments [8]. This includes combinations of surgery, RT and chemotherapy (CT) [8].

The survival rate of locally advanced HNSCC lies between 40-60 % [7] and the relapse rate is also somber. One in two patients relapse within two years after treatment, and these patients commonly only have a life expectancy of one year [7]. Risk factors of H&N cancer mainly includes heavy exposure to alcohol, tobacco and high-risk human papillomavirus (HPV) infection [7].

Radiotherapy and chemotherapy, the two most common treatments to cancer today, are while potentially life-saving also very toxic to patients. Hyperthermia treatment is being used to lower the dosage of these treatments while improving the treatment outcome. Hyperthermia means induced heating of tissue to 40-44°C for about 60 minutes[9]. Different regions of the body are more easy or difficult to apply hyperthermia to. Surrounded by a complex geometry and critical tissue such as the eyes, cerebrospinal fluid (CSF) and the spinal cord, applying hyperthermia to deep H&N tumours is more challenging compared to most other parts of the body. The benefits when succeeding are substantial. With an increased perfusion, pH and pO_2, the radio- and chemosensitivity intensifies [1]. At higher temperatures, hyperthermia also has the ability to directly kill cells [1].

Through using interference between microwaves from multiple antennas, directed heating is applied to the tumour. The combination of hyperthermia with current treatment methods has been shown to significantly increase treatment outcome of locally advanced HNSCC [10]. In a study by Valdagni et al. in as early as 1988, it was stated that the treatment results when using radiation combined with microwave hyperthermia improved treatment outcome [11]. Since then, this has been confirmed in numerous other studies [12, 13, 14, 15].

In recent years, many researchers have been working towards optimising an applicator. Applicators consist of antennas, a bolus and a frame to hold the different components in place. Both the antennas and the bolus are important parts of the applicator and when working well, they complement each other to create efficient heating. The solution created by the group that this project is a part of consists of two applicators, a separate one for tumours in the the neck and in the head. The neck applicator has already been developed, see figure 1. It uses nine antennas held together by a supporting 3D printed structure. To avoid overheating and to protect the skin of the patient, a cooling bolus is applied between the patient and the applicator. In order to start the treatment with the bolus at a comfortable temperature for the patient, and because of the low thermal conductivity of the bolus, a cooling system is applied by channels with cool water running through them. The antenna settings are, before treatment, optimised and programmed to fit the specific patient's needs. In this project, the head applicator will be developed - an essential next step in realising hyperthermia treatments for these challenging tumours.

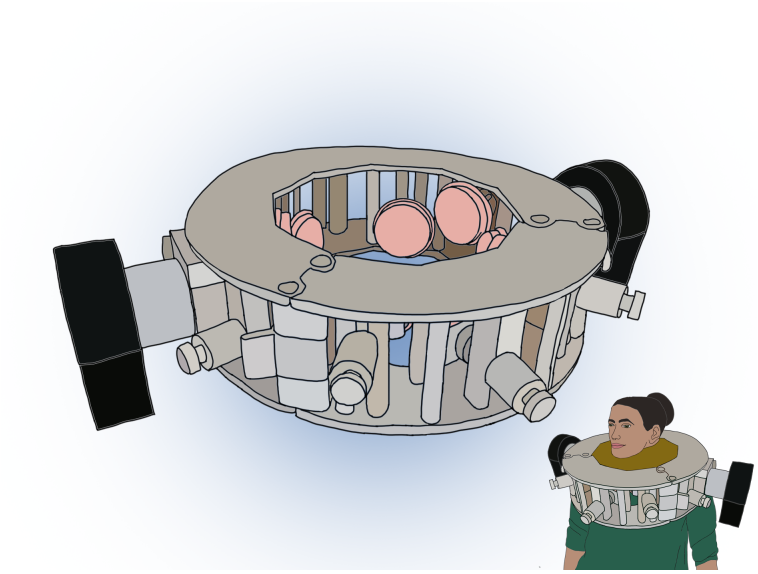

Figure 1: The neck applicator has nine antennas that can emit frequencies between 430-900 MHz. The bolus is placed between the patient and the applicator.

1.1 Aim and Limitations

The project aims to develop a head applicator for hyperthermia treatment, including design of a bolus. Different types of boli will be evaluated, including a hydrogel bolus. It will be determined if this hydrogel will be applicable for the system. The most appropriate bolus for the head applicator will be proposed. Development of the applicator includes choosing the number of antennas to be used, antenna positions, implementation of the cooling system and design of the frame.

Due to time restrictions of the master's thesis project, the completed applicator is not expected to be fabricated by the end of the thesis. Physical testing will be limited to simplified models and tissue-mimicking phantoms will be used to study the temperature distributions.

2 Background

This section will introduce theoretical background information of importance for the understanding of the project.

2.1 Hyperthermia: Then and Now

Heat and fever has for a long time been used to treat various diseases, cancer being one of them. The first recorded use of heat treatment was by an Egyptian aruspice named Imhotep (2655-2600 B.C.) [16]. A papyrus text from around 1700 B.C. describes how ancient Egyptians used hot blades and sticks to burn off breast cancer cells [16]. Almost 4000 years later, in 1866, Carl Busch published the first study showing tumour regression in a patient with high fever [17]. This, together with other studies, led to fever being induced in patients through the use of dirty bandages and malaria-diseased blood that was poured in open wounds [16]. With time, the method was refined and in 1894 the French professor d'Arsonval started treating patients with heat by placing them in a large induction solenoid, passing high frequency currents through their bodies [18].

In the beginning of the 1900s, the interest in hyperthermia was low. Heating equipment and temperature measurement techniques were insufficient and other treatment methods showed better results [16]. Hyperthermia became a hot topic again after World War II. In 1962, the American surgeon George Crile Jr. discovered that a long-lasting increase in temperature of some tumours to 42-50°C could selectively destroy them without damaging surrounding healthy tissue [17]. During this time there was a lot of research done within the field. A few years later, in 1977, Dewey et al. proved that long-term (>30 min) exposure of cells to temperatures above 40°C resulted in cell death [19]. At the same time it was shown that for temperatures above 42.5°C an increase in temperatures of the order of tenths of a degree caused significant increase in cell mortality [16], a discovery that identified the importance of accurate temperature measurements.

When microwave heating technology had been developed, a revolution in hyperthermia occured. Microwave (MW) hyperthermia allowed for more efficient and focused heating, and opened up the possibility of heating deep tumours, so-called local-regional hyperthermia. In 1939, Hollman predicted that 25 cm waves could be focused to heat deep tissues without excessively heating the skin [16]. A few years later, in 1946, the Federal Communications Commission assigned the frequency of 2450 MHz to physical medicine due to the alleged effectiveness for therapeutic applications [16, 4]. Between 1977-1983, a Danish oncologist named Jens Overgaard performed several clinical studies on the combined effect of hyperthermia and radiotherapy [16]. The results confirmed hyperthermic cytotoxicity and the benefits of combining hyperthermia with radiotherapy [9], enticing the community to further include hyperthermia in cancer treatments. The studies also pointed out the ineffectiveness of the hyperthermia devices developed at that time and the difficulties that came with heating up tissues with a built-in cooling system - blood flow [9]. The beneficial effect of combining hyperthermia to radiotherapy was recently reaffirmed in a meta-analysis done early 2019 by Datta et al. The study looked into the radiosensitivity of hyperthermia with radiotherapy (HTRT) and RT alone, concluding that there was a significant increase in radiosensitivity for HTRT as compared to RT [20]. In the 1960s to 1990s, the combined work of many researchers showed the increase in effect when certain chemotherapeutic agents were combined with hyperthermia [21]. A study by H. Kampinga in 2005 also pointed at the possibility of overcoming multi-factorial resistance to chemotherapeutic agents by the addition of heat [22].

MW hyperthermia is today widely used for therapeutic applications. One of the great difficulties of the treatment method is when it needs to be applied to deep tumours in sensitive body parts, e.g. head and neck tumours. Even when focusing the treatment on a tumour, other tissues are inadvertently heated which creates a risk for hot spots in areas with highly conducting tissue or

liquid. When this occurs, an adjusted, preferably higher, focus is required to reach the crucial temperature. There has been multiple studies looking at the effect of hyperthermia on H&N tumours. These have evaluated the effect of hyperthermia for superficial tumours (3-4 cm deep). The first system for deep-seated H&N tumours was introduced in Rotterdam, Netherlands, where the HYPERcollar system was used for clinical trials between 2007-2014 [10, 23]. This system was used for 47 patients with deep H&N tumours [10] and results showed that applying hyperthermia to RT using this system was safe and had a promising outcome [24].

An updated version, the HYPERcollar3D is now in use since 2014 [10]. This system utilises 20 patch antennas inside a metal frame, covered by a plastic bolus, and has shown improved results to its predecessor [10, 25]. The research group at Chalmers University of Technology that this thesis is a part of is developing an applicator based on the same principle - many antennas placed around the head or neck that emits MW. All other hyperthermia applicators work at one frequency, usually within the frequencies designated for industrial, scientific and medical (ISM) applications. More information about the ISM frequencies is given in section 2.5. The potential benefit of this applicator is primarily its ultra wide band (UWB) nature. To accomplish this, a different type of antennas are used. A compact self-grounded Bow-Tie antenna was developed within the research group for a UWB phased-array hyperthermia applicator [26]. The wide frequency band allows for an adapted size of the focal spot, creating adaptability in the treatment for each individual tumour. More details on different types of antennas will be given in section 2.4.

2.2 Parts of a Hyperthermia Treatment System

The starting point of hyperthermia treatments using MW starts with an Magnetic Resonance Imaging (MRI) scan or Computed Tomography, acquiring an accurate 3D patient model. This model is processed: tissues are labelled and target area is determined by a responsible clinician. The dielectric properties of each tissue are assigned and the patient model is placed inside the applicator model. Hyperthermia treatment planning (HTP) is then performed using electromagnetic (EM) simulation tools and optimising algorithms. The HTP establishes amplitude, phase and frequencies to be used during treatment.

For an accurate prediction of the treatment outcome, it is of importance that there is a high resemblance between the model position and the real patient position. The patient is therefore brought in to determine the positioning before the actual treatment occurs. If a discrepancy between the planned position and the position that can be obtained in reality is identified, the HTP needs to be altered. The hyperthermia treatment is then administered on the same day as the patient receives RT or CT. If the patient undergoes RT, the hyperthermia treatment occurs within four hours after RT. In the case of CT treatment, hyperthermia is either administered simultaneously or right after. The full hyperthermia treatment process is illustrated in figure 2.

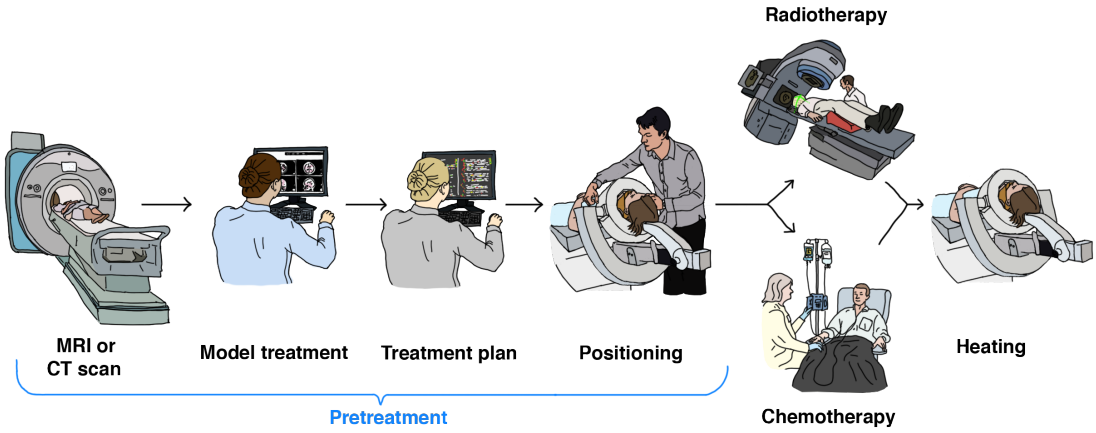

Figure 2: Steps of a hyperthermia treatment process.

Hyperthermia applicators are adapted to the body part they are used to treat tumours within. Applicators used for pelvic tumours are larger and those used for superficial tumours are usually smaller, as they can be placed on top of the area. MW hyperthermia applicators all consist of MW antennas, cooling systems to protect the patients' skin and the equipment from overheating, and a frame to hold the equipment in place. The systems also consist of temperature measurement probes and something for immobilising the treated body part. Applicators for deep tumours within the H&N region are required to surround the head and/or neck in order to create a sufficient focus. A high degree of freedom regarding the applicator parameters is beneficial for individualising the treatment for each patient's needs. This can include the possibility to adjust antenna positions or the angle that the applicator is placed at.

2.3 Interactions within Biological Tissue due to Hyperthermia

Within the frequency range used for medical applications, the effect of microwaves interacting with biological tissue is mainly an increase in temperature. Predicting this temperature increase can be done using Pennes' Bioheat equation [27]:

$$\rho c_t \frac{dT}{dt} = k\nabla^2 T + Q - \rho_{bl} c_{bl}(T - T_{bl}) \tag{1}$$

where ρ is the tissue density (kg m^{-3}), c_t the specific heat capacity (J kg^{-1} K^{-1}), k the thermal conductivity (W m^{-1} K^{-1}) and Q the heat supplied (W m^{-1}) from the heating modality (MW energy). ρ_{bl} and c_{bl}, respectively, is the density and specific heat capacity of blood. The term $\rho_{bl} c_{bl}(T - T_{bl})$ describes the heat lost through blood perfusion. Versions of this model are often applied during hyperthermia treatment planning.

The power absorption by the tissue decreases exponentially with the penetration depth [1]. Depending on the frequency used, the power deposition 1-4 cm into the tissue is only half of its original value, see figure 3 [1]. This implies that the most significant temperature increase due to hyperthermia treatment will occur in the skin and subcutaneous fat around the antenna. The cooling effect of the bolus is thereby essential, allowing a high enough temperature in the target area without overheating the superficial tissues.

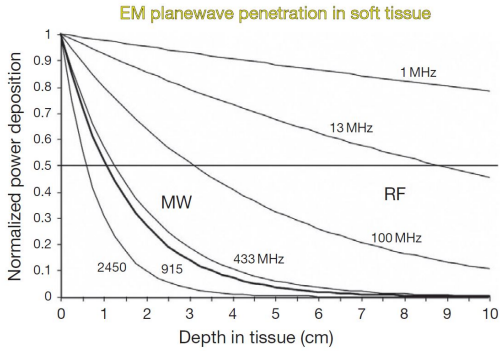

Figure 3: The power deposition as a function of penetration depth for planewave electromagnetic energy into soft human tissue [1]. Frequencies range from radiofrequency (RF) to microwaves (MW).

The microwave energy that is absorbed by the target area depends on more than the penetration depth. There are other obstacles that occur along the path to the target area. Significant changes in dielectrical properties such as the permittivity, and the geometry of the body affects the amount of energy absorbed and/or reflected along the way. Variations in the dielectrical properties, as that between air and water or between air and skin, cause dispersion of the microwaves. One way to overcome this problem is through the use of a water bolus. The bolus does not only cool the skin, but it also decreases the change in permittivity, allowing a larger percentage of the microwaves to continue in the direction of the target. Due to this, it is essential that the shape of the bolus closely follows the shape of the patient's head. If there are air gaps, diffraction will occur. When considering the geometry of the head, the chin is a potential problem area. The angle between the chin and the neck may cause cause high reflection depending on the position of the patient, dispersing many of the microwaves before they can enter the body.

The effect of adding hyperthermia to RT can be studied by looking at the linear-quadratic (LQ) model for predicting radiobiological response. Although there are multiple models available, the LQ model has been best validated by experimental and clinical data [28, 29]. The LQ model describes the surviving fraction (SF) of the tumour cells after treatment by RT as a function of radiation dose (D) [30]:

$$SF(D) = e^{-\alpha \cdot D - \beta \cdot D^2} \tag{2}$$

α and β represent the intrinsic radiosensitivity of the irradiated cells. These parameters are interesting as the $\frac{\alpha}{\beta}$ ratio describes the shape of the cell survival curve after RT. A lower $\frac{\alpha}{\beta}$ results in radiosensitation [20], meaning that the destructive effect of RT to the tumour cells is higher. By adding hyperthermia to RT treatments, the $\frac{\alpha}{\beta}$ ration decreases [20]. This is due to the ability of hyperthermia to inhibit the repair of irradiation-induced DNA damage [20].

2.4 Electromagnetism

Technology based on electromagnetism has become an essential part of today's society, not only for facilitating communication across long and short distances but also for medical applications. Electromagnetic waves with a frequency between 300 GHz – 300 MHz are called microwaves (MW) [1]. They are totally reflected by metals, while other materials such as glass and plastic, are partially transparent for them [31]. Many households include a microwave oven, which is just one example

of how these electromagnetic waves can be used for heating purposes.

Electromagnetic waves are generated by changes in potential, and consist of both an electrical and a magnetic component. These two types of waves travel orthogonal to one another and each reinforces each other. An electromagnetic wave is illustrated in figure 4.

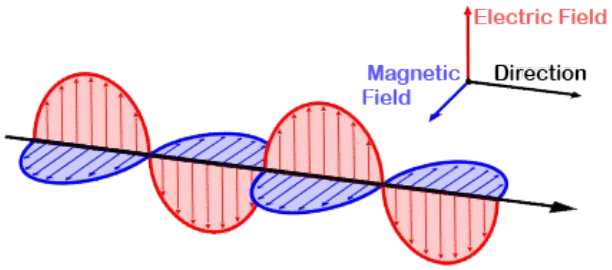

Figure 4: An illustration of an electromagnetic wave [2].

As potential differences are induced by the movement of electrons or ions, all matter to some degree generates electromagnetic waves [32]. The waves are governed by Maxwell's equations [33]:

$$
\begin{aligned}
\nabla \times \mathbf{E} &= -\frac{\partial \mathbf{B}}{\partial t}, && \text{(Faraday's Law)} \\
\nabla \times \mathbf{H} &= \frac{\partial \mathbf{D}}{\partial t} + \mathbf{J}, && \text{(Ampere's Law)} \\
\nabla \cdot \mathbf{D} &= \rho_v, && \text{(Gauss' Law)} \\
\nabla \cdot \mathbf{B} &= 0, && \text{(Gauss' Law of Magnetics)}
\end{aligned} \tag{3}
$$

E and H, respectively, are electric and magnetic field vectors and D and B are electric and magnetic flux densities. J is the electric current density vector and ρ_v is the electric charge density. These equations describe what is stated above: variations in an electric field induces a magnetic field that in turn creates an electric field. In other words, the electric and magnetic fields reinforce each other.

To transmit electromagnetic waves, antennas can be used. Two simple types of antennas antennas are monopole and dipole antennas, shown in figure 5. The frequency that these antennas can emit is determined by their length [34]. A simple broadband antenna is the Bow-Tie antenna. The name describes its shape, see figure 5. The frequencies that this antenna can emit does not solely depend on its length, it is also determined by the angle between the two triangles. This allows for a wider bandwidth compared to monopole or dipole antennas [34].

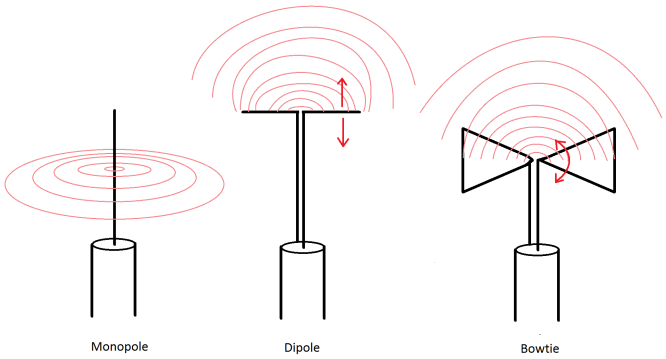

Figure 5: Three types of antennas and their radiation patterns.

Interactions between electromagnetic waves can occur in different ways, depending on the phase of each wave. The effect when two waves interact can be constructive or destructive, see figure 6. For this project when the target is deep tumours, we aim for constructive interference in the target area. By the transmissions of multiple antennas, constructive interference occurs in the target area. For an example, see figure 7, where the power absorption is higher in the centre (the target) and lower around it. As stated before, the most power is absorbed at the surface and the effect diminishes exponentially with the penetration depth. Without interaction between the microwaves, the area with the lowest absorption would be the centre. Due to constructive interference, the centre has a higher power absorbance than regions closer towards the edge. Contrary to its name, destructive interference can also be beneficial. For hyperthermia purposes this would be the case if the attenuating effect occurs outside the target area, allowing a higher temperature increase in the tumour while limiting the increase in healthy tissues.

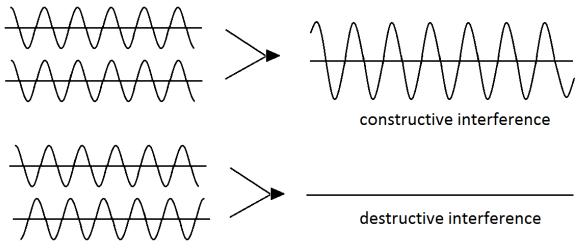

Figure 6: Types of interference between waves.

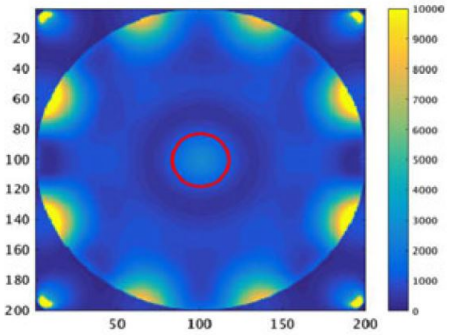

Figure 7: In a study from 2018 by Takook, Trefná and Persson, the performance of hyperthermia applicators of deep-seated tumours was evaluated [3]. 15 antennas are placed around a target area. Yellow indicates a high power absorption and blue a low. A high absorption can be seen close to the antennas that are placed along the sides. In the centre, a lighter blue colour can be seen, indicating that there is more absorption there due to the constructive interaction between the microwaves. Without this effect, this spot would have the darkest blue colour in the image.

2.4.1 Project-Specific Antennas

The antennas used for this project are designed specifically for the purpose of emitting microwaves to heat up tumours. Compact self-grounded Bow-Tie antennas that can emit frequencies between 430-900 MHz are used [26]. The design can be seen in figure 8. The antenna has a dielectric layer on top of the radiating arms (not seen in the figure) and the antenna housing is during use enclosed in water. By enclosing the antennas in water, a substance with high permittivity, their size can be reduced with the effect retained [26]. The housing of the antenna is design to avoid radiation in all directions, and aims the waves towards our target.

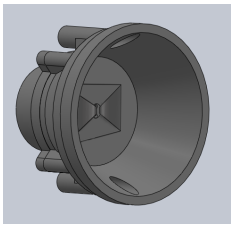

(a) Front and side.

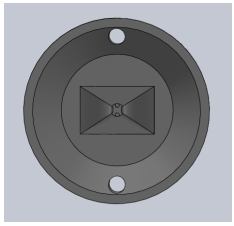

(b) Front.

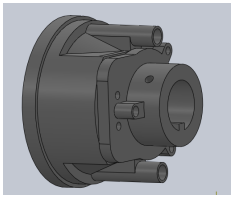

(c) Back and side.

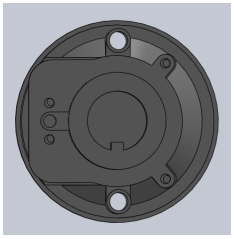

(d) Back.

Figure 8: The antenna design that will be used for this project. The antenna housing is 6.6 cm in outer diameter.

2.5 ISM Frequencies

Due to the large number of applications based on electromagnetic waves, governmental agencies have stepped in to regulate which frequencies can be used for different purposes. The Federal Communications Commission (FCC) regulates interstate and international communications by radio, television, wire, satellite and cable in the United States [35]. This agency has designated certain frequency bands for various purposes: radio, military, satellite systems etc. Some frequency bands are set aside for the industry, scientific and medical applications, the so-called ISM frequencies. The frequency bands used for ISM applications have spread around the world, setting the standard for what should be used and influencing regulations in countries around the world. The regulatory agency in Sweden is called Post- och Telestyrelsen (PTS) and utilises the same frequency bands for ISM applications [5]. The ISM frequencies can be seen in table 1.

Frequency band	Centre Frequency
13553-13567 kHz	13560 kHz
26957-27283 kHz	27120 kHz
40.66-40.70 MHz	40.68 MHz
2400-2500 MHz	2450 MHz
5725-5875 MHz	5800 MHz
24-24.25 GHz	24.125 GHz

Table 1: The ISM frequencies [4][5]. Additional frequency bands may apply in specific regions.

Due to the practicalities of being able to utilise these the ISM frequencies, this is done by most hyperthermia applicator systems. From the decision not to limit our applicator to these frequency bands, follows that the treatment room needs to be screened off. No microwaves from the treatment system with frequencies outside the ISM bands may exit the room, due to the risk of interference

with systems that these frequencies are designated for. This creates requirements on the clinical setting, but also facilitates a higher degree of freedom regarding the capabilities of the applicator.

2.6 Thermodynamics

In the process of designing a water bolus that can efficiently cool the skin during hyperthermia treatment, there are many aspects to consider. There are different modes of energy transfer and numerous parameters that affect how much heat can be removed from a given region. Rather than studying Pennes' bioheat equation which is used for biological tissue, different equations need to be applied for this case. For the purpose of understanding the evaluation of boluses that will be performed, some basic principles of thermodynamics are given here.

One of the main modes of energy transport between objects is convective heat transfer. Convection occurs is heat transfer and occurs between a solid and a moving fluid. It can be either forced or natural [36]. Forced convection is when e.g. a pump is used, such as in the evaluation done in this project. Newton's Law of Cooling describes the heat transfer per surface unit through convection [36].

$$q = h_c A(T_{\text{solid}} - T_{\text{liquid}}) \tag{4}$$

Where q is the heat transferred per time unit, h_c convective heat transfer coefficient, A the actual heat transfer area and T the temperature of the surface and bulk fluid, respectively [36]. From this equation, it is clear that a larger area and higher temperature difference between the solid and liquid will result in more heat transferred per time unit.

Conduction is another main mode of energy transportation. It occurs primarily between solids. Conduction is described by Fourier's Law [37].

$$q = -kA\frac{T_{\text{solid1}} - T_{\text{solid2}}}{dx} \tag{5}$$

The variables are the same as in equation 4. Radiation is the third main mode of energy transportation, and does not require a medium to transfer energy. The equation describing thermal radiation is [38]:

$$q = e\sigma A(T^4_{\text{radiator}} - T^4_{\text{surrounding}}) \tag{6}$$

Where σ is the Stefan Boltzmann constant and e the emissivity (1 for an ideal radiator).

One other central concept in thermodynamics is heat capacity. It describes the ratio of heat absorbed by a material to the temperature change, and is commonly measured in calories per °C.

3 Evaluation and Design of Water Bolus

The first part of the project involves evaluation and design of the water bolus (WB) to be used with the applicator. The potential of a novel, hydrogel-based WB [39] was studied in contrast to the standard solution in terms of a water-filled plastic bag.

The two main, and very important, functions of the bolus are cooling the tissue surface and to couple the EM waves into the high permittivity of tissue [40]. Generally used for hyperthermia purposes are plastic bags filled with water. The water is circulated throughout the bolus to increase the heat transport away from the heated superficial tissue. Different types of plastic can be used for a bolus of this type, which from now on will be called a waterbag bolus. Common problems with waterbag boli include leaking and difficulty to adhere to the patient's contour. The newly developed hydrogel bolus consists of 99% water and 1% xanthan/locust bean gum (LBG)/agarose, which creates a soft and deformable gel [39]. The ternary system thereby overcomes the problem of leaking while allowing a closer fit around the patient. Attempts to create an active cooling system for the hydrogel bolus have been made [41]. It provides a promising option to the traditional waterbag bolus, but is in need of testing before implementation.

Three types of boli will be tested during this evaluation: a hydrogel without active cooling, a hydrogel with active cooling and a waterbag bolus. The cooling ability of the boli will be evaluated through studying the temperature change over time with different setups. After the cooling effect of the boli has been determined, they will be assessed based on multiple criteria of importance for hyperthermia treatment. If the waterbag bolus is the favorable option, a material evaluation needs to be performed.

Before the physical experiments were performed, simulations of the first experiment were done. With accurate results, simulations reduce the resources that are required for experimental validation. Performing simulations in place of physical experiments is thereby something to strive towards when results of adequate quality can be produced. The heat transfer rate of the bolus and phantom was studied and the results were saved for comparison with experimentally obtained data. The aim of the simulation was in this case partly to predict the behaviour of the model, but mostly to evaluate the accuracy of the simulations for future reference.

3.1 Experimental Setup

The experiments will be done for two different cases. First, the cooling effect will be studied without an active heat source present, whereupon a MW antenna will be added. The simplest experiment, with no heat source, involved each bolus placed on top of a muscle phantom. The recipe for the phantom is given in appendix A. The temperature decrease over two hours, double the time of a normal hyperthermia treatment session, was observed. When the MW antenna was added, the experimental setup was adapted slightly. Each bolus was, one at a time, again placed on a muscle phantom, but an extra muscle phantom was placed below to avoid potential reflection from the table. The experimental setup for each experiment can be seen in figure 9.

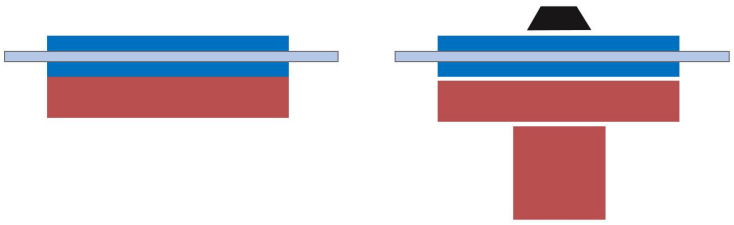

Figure 9: The experimental setup seen from the side, without (left) and with (right) an external heat source. The heating source was a microwave antenna. Blue represents the bolus, red the phantom, grey the silicone tube and black the antenna.

3.2 Simulation of Bolus Effect

The effect of the three different bolus systems was simulated using SOLIDWORKS® Flow Simulation. The simulation was only performed for the first experiment, without external heating, due to time limitations. The material properties and temperatures were set to be as similar to the real values as possible. Due to variations in room and water temperature between experimental sessions, the simulation was rerun after the physical experiments to make the comparisons between experiment and simulation more accurate. The different parameter settings for the simulations can be seen in table 2 and 3.

	Hydrogel	Hydrogel with cooling	waterbag
Air (°C)	22	22	24
Bolus (°C)	6	6	10
Phantom (°C)	21	21	24
Flowing water (°C)	-	13	10

Table 2: The initial temperatures that were used for different materials to obtain the simulated results from the experiment without MW radiation. They were adjusted to correspond to the real experimental temperatures, which is why they differ between each other. Remaining relevant settings that were the same for all boli were: Pressure was 101325 Pa, Heat conduction was considered in solids, the simulation was time-dependent, no gravity or radiation was considered. For simulations using flowing water a water flow of 1 g/s was used with only laminar flow.

	Hydrogel	Muscle Phantom	Silicone	Water
Material type	Solid	Solid	Solid	Liquid
Density (kg/m^3)	998	1090	1150	998*
Specific heat (J/(kg·K))	4100	3686	2200	4184*
Thermal conductivity (W/(m·K))	0.62	0.49	0.27	0.60*
Conductivity type	Isotropic	Isotropic	Isotropic	-
Electrical conductivity	Dielectric	Dielectric	Dielectric	-
Dynamic viscosity (mPa·s)	-	-	-	1.0014*

Table 3: Dielectrical properties used to define materials for simulations. The silicone material properties were used for the tube and the encasing of the waterbag. *Varies with temperature, given value is at 20°C.

The results from the simulations can be seen in figure 10.

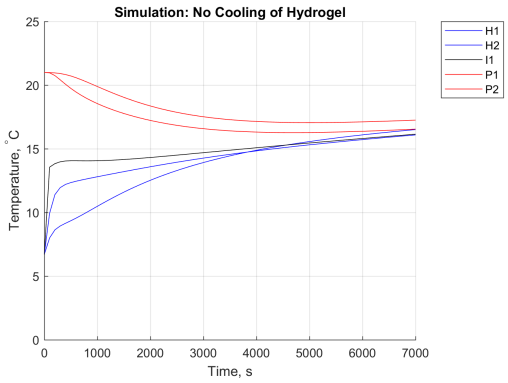

(a) Simulation results of hydrogel with no cooling.

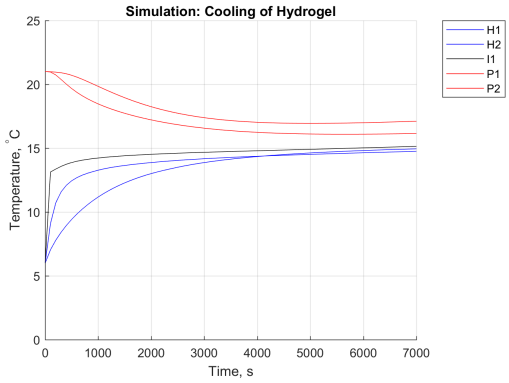

(b) Simulation results of hydrogel with cooling.

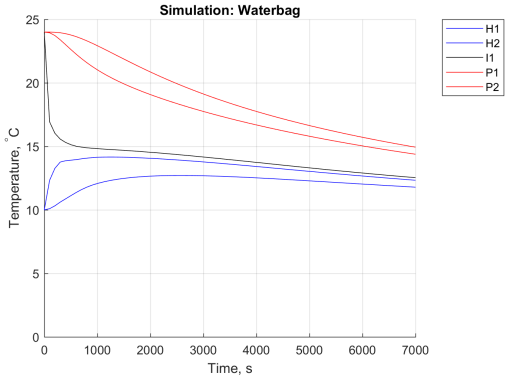

(c) Simulation results of waterbag.

Figure 10: The simulated results for the experiment without external heating. The temperature change over time is showed for the hydrogel without cooling 10a, the hydrogel with cooling 10b and the waterbag 10c. H1, H2, I1, P1 and P2 represent temperature probe positions, see figure 11.

3.3 Bolus Evaluation Without MW Antenna

The boli were first evaluated by comparing their ability to cool a muscle phantom. They were placed on top of the phantom and the heat exchange was studied for two hours. The temperature was measured using temperature probes. A detailed experimental setup can be seen in figure 11, together with the initial temperatures.

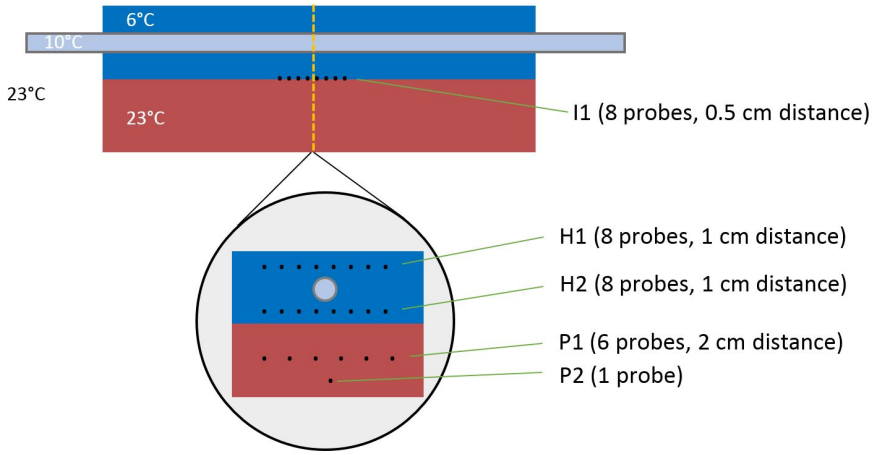

Figure 11: Experimental setup. Blue colour (upper block) represents the hydrogel, gray is the tube (in cooling experiment this is filled with water) and red (bottom block) is muscle phantom. The black dots represents the temperature probes. The following abbreviations are used to label the probes: H - hydrogel, P - phantom, I - intersection.

The real setup with the hydrogel is shown in figure 12a and 12b. The experimental setup with the waterbag remained the same as with the the hydrogel experiments, but with the waterbag instead of the hydrogel. At the start of the experiment, the waterbag was filled with 10°C water circulating through the ports. Due to difficulties measuring the temperature inside of the waterbag, probe H1 measured the inlet water temperature and probe H2 measured the outlet water temperature. The other probes remained in the same position. For the real experimental setup with the waterbag, see figure 12c.

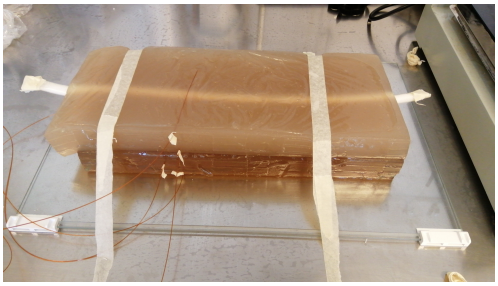

(a) Hydrogel with no cooling. Tube has no water circulating.

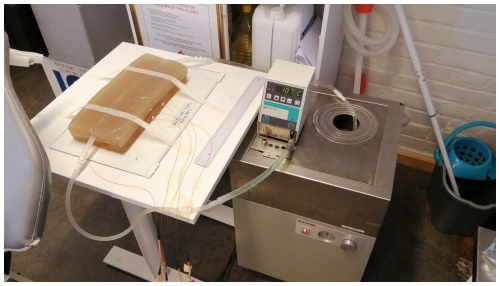

(b) Hydrogel with cooling. Water is circulating through the tube.

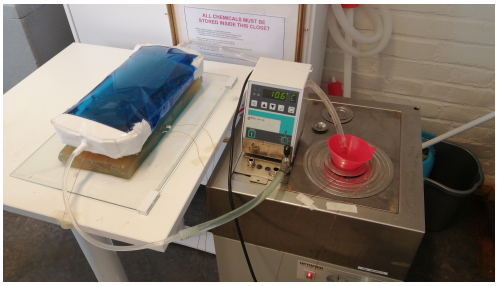

(c) waterbag with circulating water.

Figure 12: Real experimental setup for the experiment with no MW radiation.

3.3.1 Materials

The materials used for this experiment are listed below.

- Hydrogel (5 cm x 16 cm x 36 cm) with tube (10 mm inner diameter, 12 mm outer diameter, material is silicone)
- Waterbag (5 cm x 16 cm x 36 cm) made of about 0.5 mm plastic sheets, glue, inlet and outlet ports and duct tape
- Muscle phantom (5 cm x 16 cm x 36 cm)
- Water cooling system, pump and tubes
- Fiber optic probes from FISO Technologies 11).

The recipe for the hydrogel and phantom can be found in Appendix A. A rectangular mould was used and a silicone tube was placed inside. The tube was filled with sugar to avoid it collapsing from the weight of the hydrogel. Although the same mould was used for the hydrogel and the phantom, the hydrogel deformed after being outside the mould, this deformation from the original size can be seen in the photo from the real experimental setup, see figure 12a.

The fiber optic probes were used to measure the temperature during the experiments. These work well for MW hyperthermia applications as they are immune to electromagnetic interference [42]. The probes were calibrated through the method developed by Alhede et al. in 2019 [43].

3.3.2 Results from Evaluation without MW Antenna

The results of the experiment using the hydrogel without cooling water can be seen in figure 13.

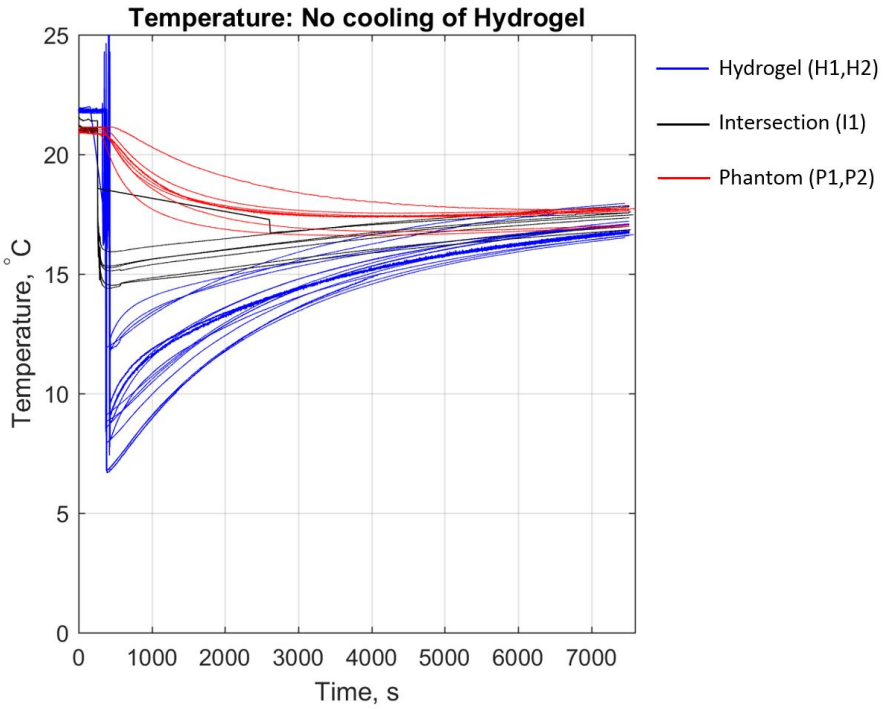

Figure 13: The experiment done without external cooling. The hydrogel started at about 6.7°C and the phantom at room temperature, 21°C.

Without cooling, the hydrogel temperature slowly increased towards the temperature of the phantom and the surrounding air. The spikes in the data are due to placement of the hydrogel and the probes inside it, causing rapid temperature changes. The different measurement points converge towards around 17°C, with a slight incline. The incline indicates that steady state has not been reached, and that the temperature at this state will be higher.

The results from the experiment using the hydrogel with active cooling is shown in figure 13. Due to difficulties during the experiment, more circulating water had to be added to the cooling system. The lowest temperature of the tap water that could be added was 17°C, unfortunately this resulted in warming the cooling water during the experiment.

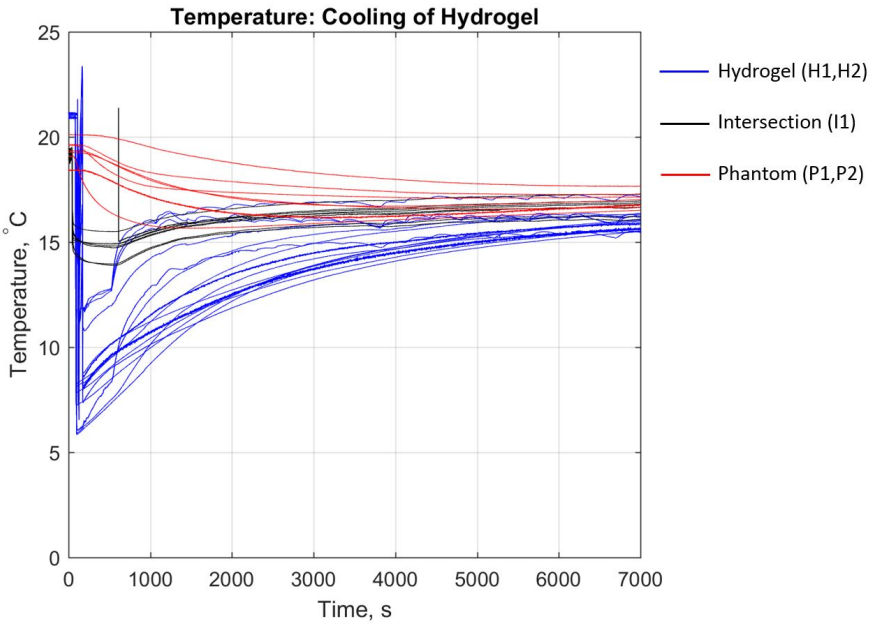

Figure 14: The experiment done with external cooling water at around 17°C. There is no clear incline at the end, implying that a steady state will be reached within the reached temperature limits (about 16°C).

The results of the same test, but with a waterbag instead of the hydrogel can be seen in figure 15.

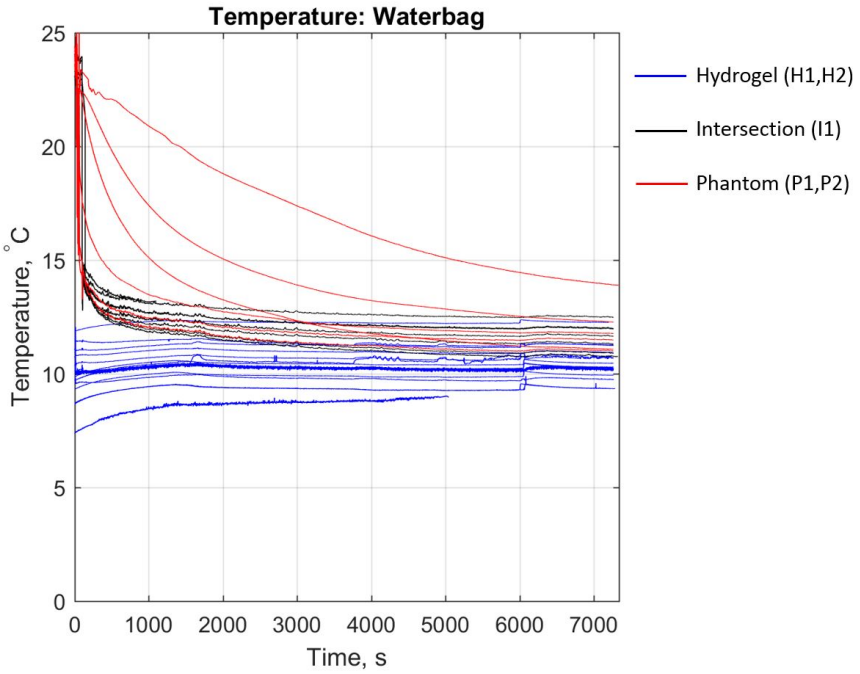

Figure 15: The room temperature this day was higher than last time, so the phantom started at around 24°C rather than 21°C. The inlet water varied between 10 and 11°C.

The phantom temperature decreased rapidly in the areas close to the waterbag and more slowly in the parts further away.

When comparing the results of the experiments done without radiation, it can be seen that although the intial temperature of the waterbag is higher (10°C compared to 6°C) and the decline therefore is slower, the phantom temperature of the waterbag drops below the temperature of both hydrogels. The graphs are overlaid in figure 16. A clear difference can be seen between the waterbag data and the hydrogels. It is hard to distinguish between the two hydrogels until at the end of the two hours.

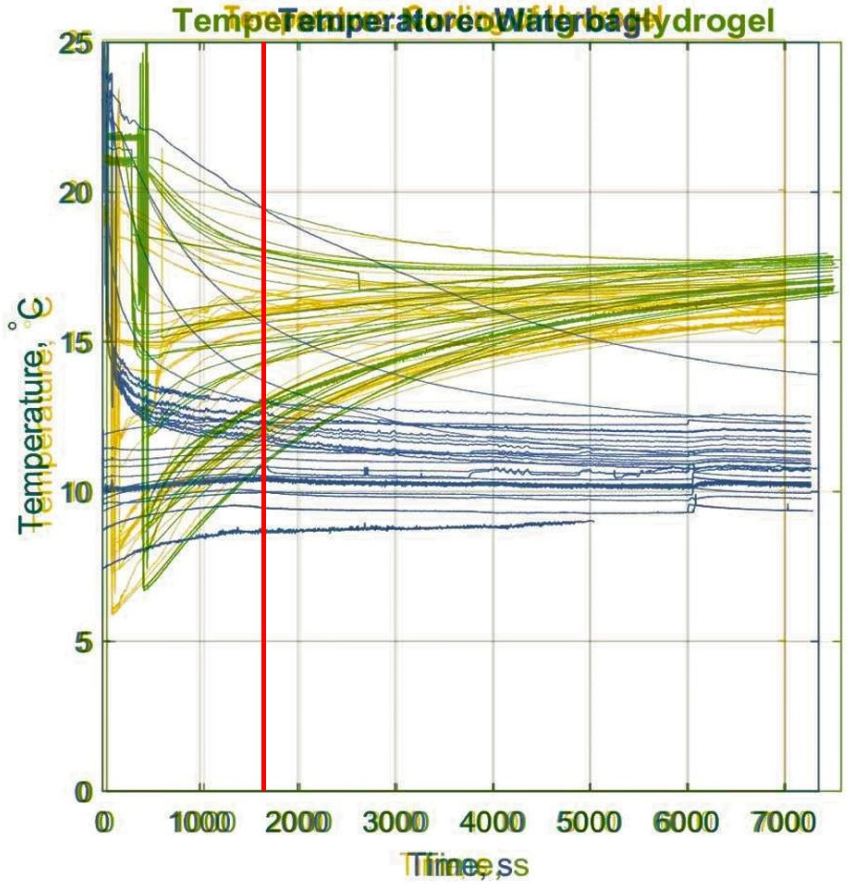

Figure 16: The three graphs are placed on top of each other for comparison. The green is the hydrogel without cooling, the yellow is the hydrogel with cooling, and the blue is the waterbag. The red line indicates where the phantom of the hydrogel is lower in temperature than the phantom of the hydrogels. This occurs after 26 min (1600 s).

3.4 Bolus Evaluation with MW antenna

This experiment was run using a similar setup as the experiment without radiation, but with an antenna radiating on top and an extra phantom at the bottom to avoid reflection from the table surface. The temperature probes were also placed differently. The Bow-Tie antenna was used for radiating microwaves. The wavelength was determined through examining the scattering parameters. The S11 curve can be seen in figure 17 and describes how much of the radiated microwaves is received back by the same antenna. The detailed setup is presented in figure 18.

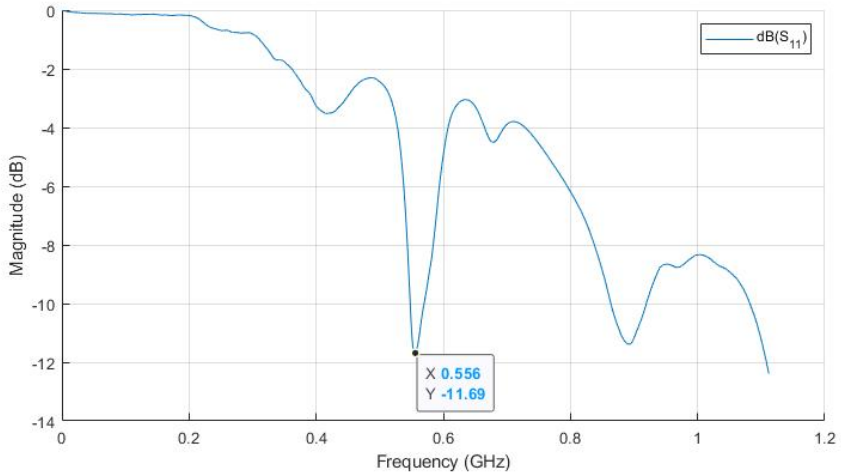

Figure 17: S11 measurements for the specific Bow-Tie antenna that was used. For the frequency 556 MHz, the S11 parameter of the antenna was below -10 dB.

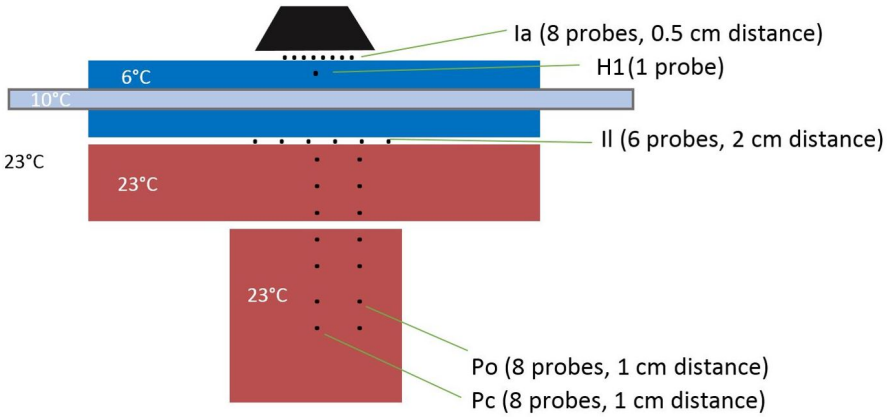

Figure 18: Experimental setup. Blue colour (upper block) represents the hydrogel, gray is the tube (in cooling experiment this is filled with water) and red (bottom block) is muscle phantom. In this experiment there was, apart from the rectangular phantom, an extra phantom in the shape of a cylinder (the shape is not of importance). It was placed there for the purpose of absorbing excess radiation. The black is the antenna radiating at 556 MHz. The black dots represents the temperature probes. The following abbreviations are used to label the probes: Ia - Intersection at antenna, H - Hydrogel, Il - Intersection lower (between hydrogel and phantom), Po - Phantom offset from middle, Pc - Phantom centre.

The wavelength used for the experiment was 556 MHz, as this was the minimum S11 value. The antenna was placed on top of the hydrogel, in the centre. The effect used was 120-130 W. Cool

water was circulated inside the antenna as well as the amplifier to avoid overheating.

The real setup with the hydrogel is shown in figure 19a and 19b. For the real experimental setup with the waterbag, see figure 19c. The material used is given in section 3.4.1.

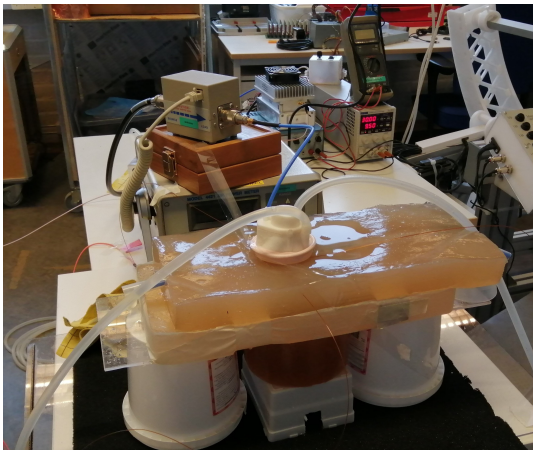

(a) Hydrogel with no cooling. Tube has no water circulating.

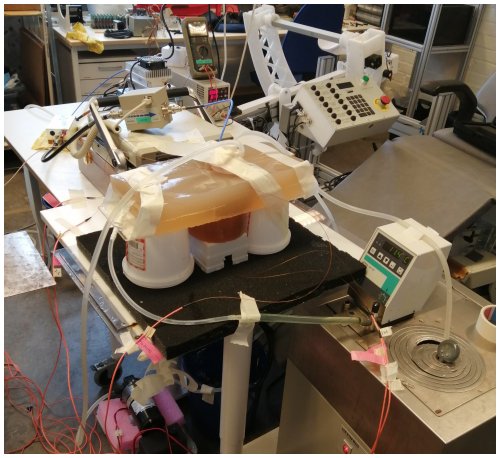

(b) Hydrogel with cooling. Water is circulating through the tube.

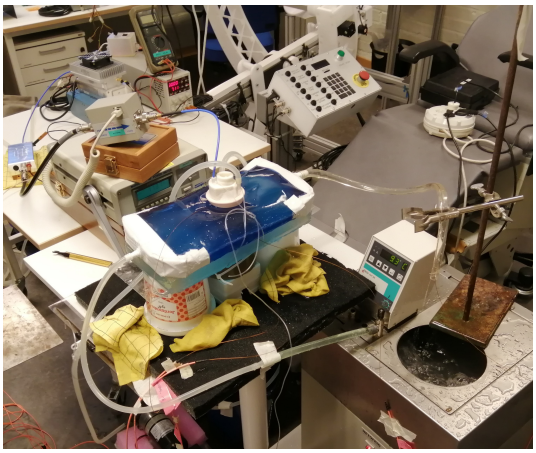

(c) waterbag with circulating water.

Figure 19: The real experimental setups for the experiments with MW radiation. The setup, with the exception of the bolus is the same for all versions, but what was available to keep the antenna in place varied. The rags in figure 19c were used to absorb leaking water.

3.4.1 Materials

For this part of the experiment, more equipment had to be used. The material is listed below:

- Hydrogel (5 cm x 16 cm x 36 cm) with tube (10 mm inner diameter, 12 mm outer diameter, material is silicone)
- Waterbag (5 cm x 16 cm x 36 cm) made of about 0.5 mm plastic sheets, glue, inlet and outlet ports and duct tape

- Muscle phantom (5 cm x 16 cm x 36 cm)
- Water cooler, pump and tubes for circulating water through the bolus
- Fiber optic probes from FISO Technologies for temperature measurements
- Open-ended coaxial dielectric probes (Agilent Technologies, USA) and vector network analyzer (VNA) (Agilent Technologies, USA), for S11 measurements
- Compact self-grounded Bow-Tie antenna
- Oscillator
- Preamplifier
- Amplifier
- Pump, tubes and bucket with cooling water for amplifier
- Pump, tubes and bucket with cooling water for antenna

Recipes for the hydrogel and muscle phantoms are given in Appendix A. A diagram of the electrical setup can be seen in figure 20.

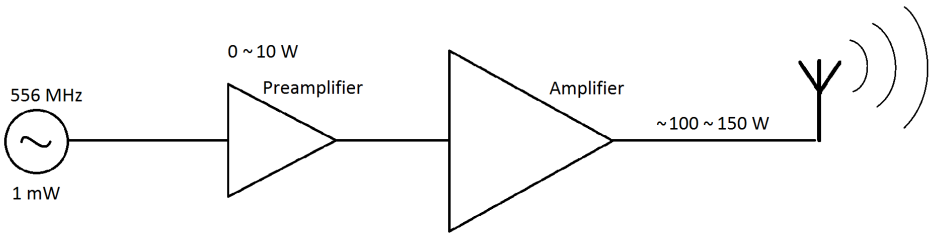

Figure 20: The electrical setup during the experiment with MW radiation.

3.4.2 Results from Evaluation with MW Antenna

The results of the experiment performed with an antenna radiating microwaves for the hydrogel without cooling are presented in figure 21.

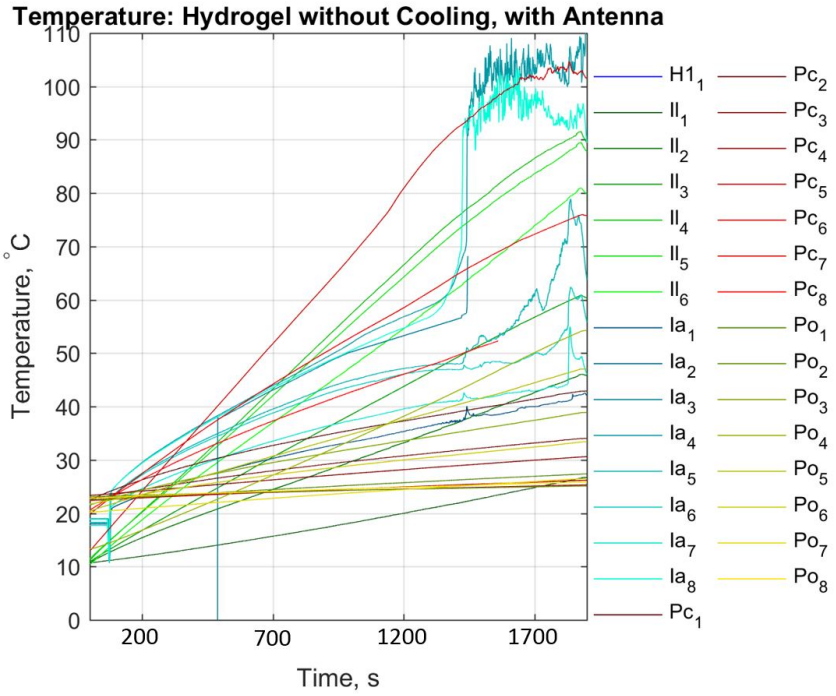

Figure 21: The experiment done with the hydrogel and no external cooling. At around 2200 seconds, the radiation was turned off due to having reached harmful temperature levels for the temperature probes used.

When the experiment was performed with the hydrogel without external cooling, the phantom was heated to such high temperatures (>100°C) that the experiment had to end early. It took 32 minutes for the radiation to heat up the phantom, through the cooling phantom, to above 100°C. When the experiment was stopped, there were no externally visible damage to the hydrogel or phantom. As the setup was disassembled, it was found that inside, in the path of the radiation, was a hole where the phantom had melted of about 3 cm in diameter going all the way through it. The hydrogel had also melted and had a hole, although not all the way through. There was no damage to the extra phantom in the bottom. The damaged hydrogel and phantom can be seen in figure 22.

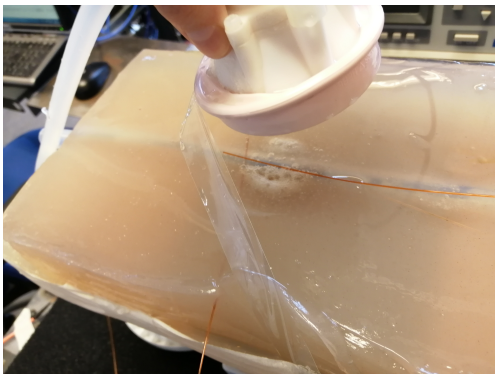

(a) The damage to the hydrogel.

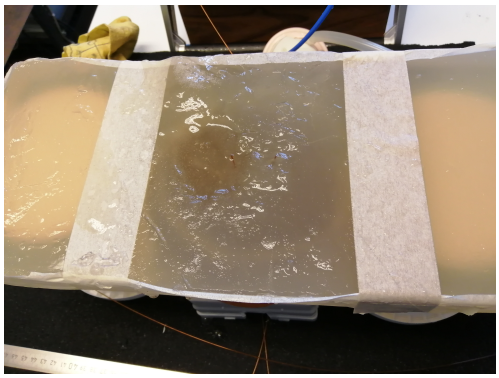

(b) The damage to the phantom.

Figure 22: The bolus and phantom was damaged due to overheating when the hydrogel without external cooling was used.

When the experiment was performed using the hydrogel with external cooling instead, see figure 23, it could be carried through the whole hour. This is what is expected in a real patient treatment. At the end there was no externally visible damage to neither bolus nor phantom. When disassembled a hole about 2 cm in diameter was found in the phantom. The hydrogel was also damaged, with a hole about 1 cm in diameter on the side that faced the phantom. On its other side, a small indent from where the antenna was placed could be seen. The highest temperature reached was in probe number Pc_6, the probe in the top of the phantom where the hole was.

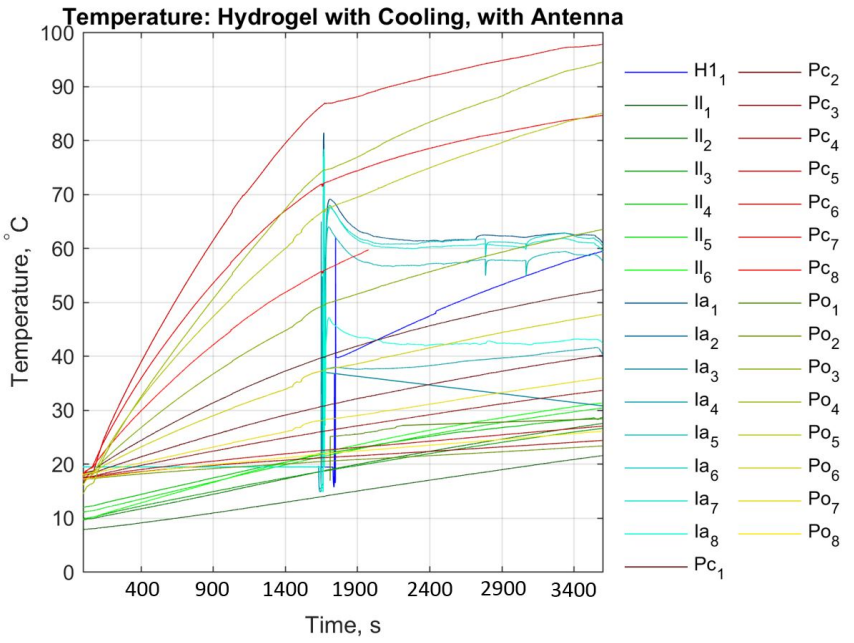

Figure 23: The experiment done with the hydrogel and external cooling. The highest temperature reached was 97°C after one hour, in the central phantom probe number 6 (Pc_6). The probes under the antenna had not been placed and were inserted after half the time had passed, giving rise to the large spike in the graph.

When the cooling system used was the waterbag, the experiment could be run for the full hour with the temperature remaining below 75°C, see figure 24. The maximum temperature was obtained in probe Pc7, in the top part of the phantom. No external damage was visible at the end, and no damage was found to neither bolus nor phantom when the experiment was disassembled. There was an indent in the hydrogel after where the antenna had been placed, see figure 25. During this experiment, there was leaking which required substantial attention.

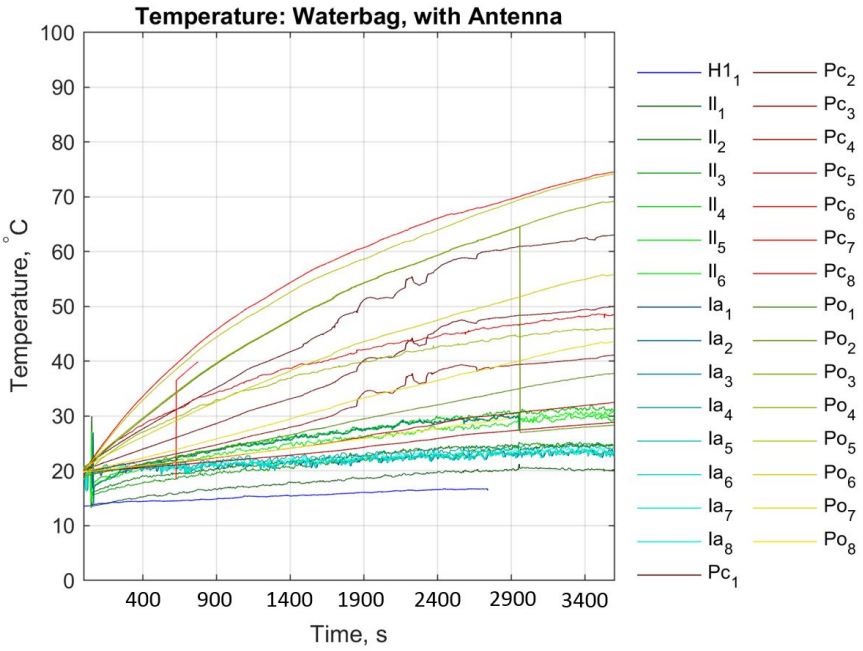

Figure 24: The experiment done with a waterbag where water was circulated an opening and outlet at each long-side of the rectangular bag (same positions as the in- and outlets of the hydrogel with cooling). The experiment reached a maximum at the end of the 1h radiation period, at 75°C in probe Pc_7.

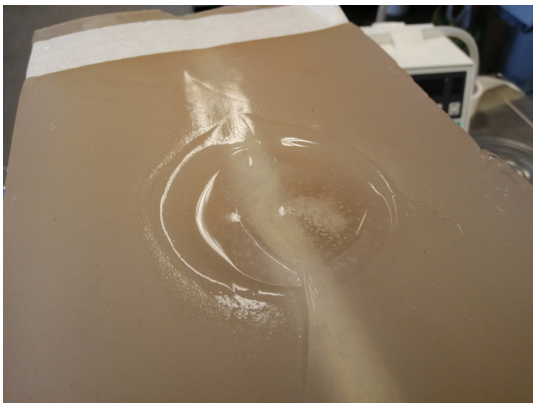

Figure 25: The indent made from the antenna in the hydrogel.

The evaluation of boli has shown that the waterbag is more efficient for cooling the phantom compared to the hydrogel, both with and without external cooling of the hydrogel. It is also important to consider limitations related to construction and fit to the patient when choosing a bolus type. This will be considered using a Kesselring matrix.

3.5 Temperature Sensation

The temperature of the bolus water is an important factor regarding the effectiveness of hyperthermia treatment. Temperatures used for the bolus commonly ranges between 25-40°C, where the higher temperatures are used for superficial tumours. Lower temperatures are needed the more centralised the tumour is in the body. For deep-tumour applications, temperatures below 37°C are mostly used. In the experiments done in this project, the bolus temperature ranged between 6-12°C, significantly lower temperatures compared to what is normally used. When utilising the hydrogel bolus where the cooling ability is less effective, a low initial temperature is required to obtain satisfactory results. Simultaneously, patient comfort has to be considered which restricts what temperatures can be used.

To facilitate future work looking into the initial temperature of the bolus, and to consider whether the hydrogel can have the initial temperature required to function well, a small study with three healthy volunteers was done. Plastic bags filled with water between 7-30°C were placed on the participants' face and neck, one body part at a time. The participant then rated the comfort according to a given scale from 1-10, where a 10 was an extremely comfortable experience and a 1 was unbearable and the experiment had to be interrupted. The bags of water were kept on the skin for five minutes and about 30 minutes was given for recovery between sessions. The results are shown in figure 26.

		7	10	15	22	25	30
Subject 1	Face	5	4	5	6	6	6
	Neck	5	6	6	6	7	7
Subject 2	Face	-	6	5	7	8	9
	Neck	-	5	7	7	7	8
Subject 3	Face	3	3	3	6	6	7
	Neck	4	4	4	5	6	6

10	Extremely comfortable
9	Very comfortable
8	Pretty comfortable
7	A little comfortable
6	Alright
5	A little uncomfortable
4	Pretty uncomfortable
3	Very uncomfortable
2	Extremely uncomfortable
1	Had to remove

Figure 26: The results of temperature sensation measurements on three participants.

The results indicate that a temperature above 20°C was mostly comfortable and could, after further testing, probably be used as a starting temperature of the bolus. If lower temperatures are required for treatment effectiveness, as in the case of the hydrogel, none of the participants had to remove the waterbag for the measured temperatures which indicates that lower temperatures are bearable, although not comfortable for patients. The participants did describe numbness in the areas where the bag of water that was 7°C had been after the five minutes, signalling that this temperature might be problematic for the actual treatment time of one hour.

Keeping in mind that this data is not representative of a larger group of people, it simply gives an idea of what temperatures can be used. Based on this, a starting temperature of 25°C would be comfortable for patients and 15°C is bearable if a low temperature is necessary.

3.6 Waterbag Bolus Material Evaluation

Materials to be used for the waterbag were evaluated through literature studies, practical tests and previous experience from research group members. After data had been collected and tests had been performed, they were evaluated using a Kesselring decision matrix. First, the bolus type was evaluated based on the results from the experiments above as well as other factors. The results can be seen in figure 27. The weight shows the significance of each criteria, where 1 is little significant

and 5 is very significant. The total score for each criteria is the weight multiplied by the grade. The hydrogel with and without active cooling and the waterbag are compared to an ideal bolus.

Criteria		Bolus type								
		Weight	Ideal		Hydrogel (only)		Hydrogel with tube		Waterbag	
			Grade	Total	Grade	Total	Grade	Total	Grade	Total
A	Construction time	1	5	5	3	3	3	3	2	2
B	Construction complexity	2	5	10	3	6	2	4	3	6
C	Durability	3	5	15	2	6	2	6	4	12
D	Maintenance	4	5	20	3	12	3	12	5	20
E	Fit to patient	4	5	20	4	16	4	16	3	12
F	Effective cooling	5	5	25	1	5	3	15	5	25
G	Leakage	3	5	15	5	15	5	15	3	9
H	Usability	3	5	15	3	9	2	6	5	15
I	Simulation results	2	5	10	4	8	4	8	4	8
Total			120		71		78		101	
Total/Ideal			1		0,59		0,65		0,84	
Ranking			-		3		2		1	

Figure 27: Evaluation of bolus types based on previous experimental results and other relevant factors. The total of each criteria is the weight multiplied by the grade. The results show that the best option to move forwards with is the waterbag type bolus.

The evaluation shows that the best bolus to move forwards with is the waterbag type bolus. Although the hydrogels perform better in regards of no leaking, and fit to patient contour, the waterbag is significantly more efficient at cooling. Since cooling ability hold more importance, the waterbag remains the most favourable option. The next step is evaluation of different material options for the bag. Prototypes were constructed and the results evaluated in another Kesselring matrix, seen in figure 28. Prototypes from plastic construction foil, latex spray and liquid silicone existed before this project. A latex sheet and a silicone sheet prototype was constructed during this project, these can be seen in Appendix B.

Criteria		Material											
		Weight	Ideal		Construction foil, plastic		Latex sheet		Latex spray		Liquid silicone		Silicone sheet	
			Grade	Total	Grade	Total	Grade	Total	Grade	Total	Grade	Total	Grade	Total
A	Construction time	1	5	5	5	5	4	4	1	1	1	1	3	3
B	Construction complexity	3	5	15	5	15	3	9	2	6	2	6	4	12
C	Leakage	5	5	25	2	10	1	5	5	25	1	5	4	20
D	Durability	4	5	20	3	12	4	16	4	16	2	8	5	20
E	Scent	2	5	10	5	10	3	6	2	4	5	10	5	10
F	Elasticity	5	5	25	1	5	5	25	5	25	4	20	2	10
G	Price	2	5	10	5	10	4	8	3	6	2	4	1	2
Total			110		67		73		83		54		77	
Total/Ideal			1		0,61		0,66		0,75		0,49		0,70	
Ranking			-		4		3		1		5		2	

Figure 28: Evaluation of waterbag bolus materials. The total of each criteria is the weight multiplied by the grade. The results show that the best option is the latex spray.

The evaluation shows that, for this purpose, the best of the evaluated materials is latex spray. The construction processed for this bolus can be found in Appendix C. The latex spray waterbag bolus can be seen in figure 29.

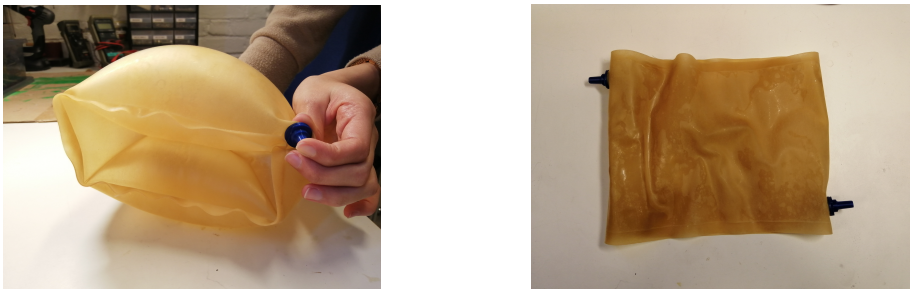

Figure 29: The bolus type that through evaluation was shown to be the best option to use. A waterbag bolus made from latex spray. Inflated and deflated. Water is circulated through the blue ports at each side of the bolus.

3.7 Bolus Design

Based on the experimental results obtained from the bolus evaluation, a waterbag-type bolus is the most efficient. The material most appropriate, based on the material evaluation, is liquid latex that can be sprayed onto a surface. This should be created over a concave surface to decrease possible folding in the material when applied on the patient. Due to the complex shape of the human neck-and-head region and the limitations of the evaluated materials, two boli should be used. One to be placed around the neck and a second one, wider, to be placed on top of the neck bolus and over the face/head of the patient. See figure 30. Water should be circulated in each one through the ports attached to the ends. With more experience in producing these types of boli or more complex equipment, the goal will be to have only one bolus that has an asymmetrical shape, following the body closely.

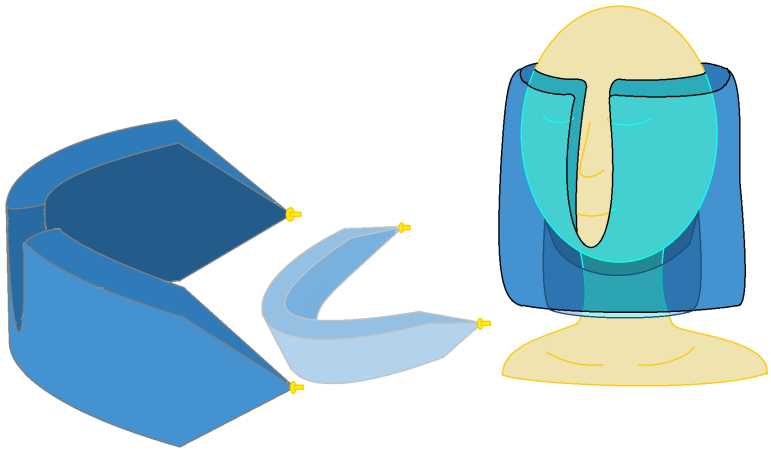

Figure 30: Bolus design to be used for the head applicator. The yellow items at the ends of the boli are ports for inlet and outlet water, where water is circulated.

4 Antenna Applicator Design

The frame needs to be designed in a way to allow for an as effective treatment as possible. This requires consideration of antenna placements, bolus position, upper body and head immobilisation and ability to hold all the necessary tubes and cords. All of this will be discussed further later on in this section.

Other than the ones considerations already mentioned, there is also a need to acknowledge the practical limitations that exist. The available 3D printers are not large enough to print a rounded shell for the applicator, and the hard plastic sheet that made up the material for the neck applicator is flat. Due to these factors, a similar design to the neck applicator, see figure 1, will be used. The starting design for the applicator is thereby two flat plates from the large plastic sheet, held together by 3D printed pins and screws.

4.1 Head Support and Immobilisation

To assure correct patient positioning and restriction to movement during the treatment, some type of holder and pillow is needed. In radiotherapy, foam pillows for the neck and head are often used for this purpose. Another option is a vacuum bag. It has small beads and after a patient places their head in the correct position, the bag is vacuum sealed to keep its shape. A bigger version of this bag can be used to keep the shoulders and upper back in place as well. The two options are shown in figure 31. Since the vacuum bag has the ability to immobilise the entire upper body, this is the preferred option.

(a) Foam pillows used to keep patients' heads in place. A pillow fitting the specific patient is chosen by their physician. [44]

(b) Vacuum bag used to immobilise a patient's upper body. [45]

Figure 31: Two options for immobilising patients during treatment.

In order to account for the space required by the immobilising pillow, the applicator cannot be a full circle as in the case of the neck applicator. Head tumours are located in the mouth and nose region, which makes the front of the head most relevant for microwave radiation. The spine is a critical tissue, and care should be taken to minimise heat in this region [23]. The design of the frame can be seen in figure 32.

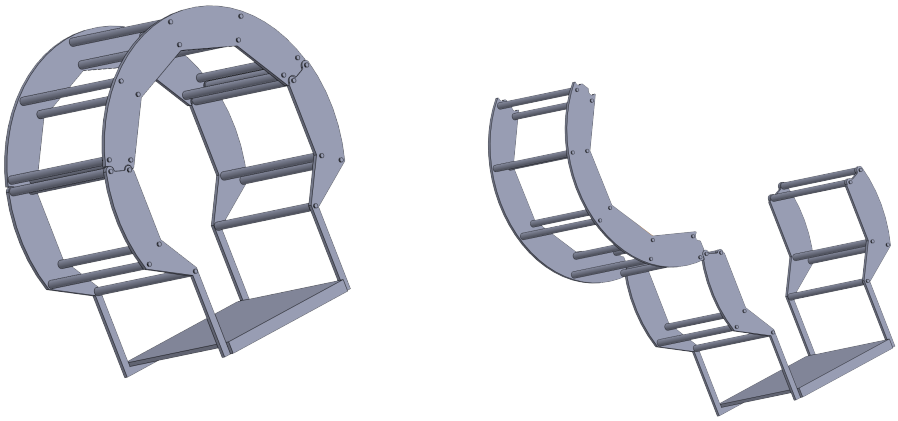

Figure 32: The design of the head applicator frame.

Positioning will be aided by the positioning machine seen in figure 33 and small motors that are attached to the antennas.

Figure 33: A device used to accurately position the applicator.

4.2 Number of Antennas and Their Placement

The number of antennas that should be used for hyperthermia varies depending on the size of the target area and the frequencies to be used. It also depends on the accuracy required of the focus. A study from 2018 by P. Takook, M. Persson and H. Dobšíček Trefná showed that an increased number of antennas was for most tumour types beneficial compared to a lower number [3]. A higher number of antennas operating at higher frequencies increased the power absorption in the tumour [3]. Care also has to be taken not to place antennas too close, causing cross-coupling. A study done by C. Rigato in 2013 has assessed different options for placing antennas in head applicators [46].

For head regions, it was found that one ring does not provide sufficient energy, leaving no focus in the centre [46]. Two different two-ring applicators were studied: one with 6 antennas and one with 8 antennas per ring. Two rings with 8 antennas performed better, the sum from each antenna is higher while still keeping enough distance between the transmitters to avoid cross coupling [46]. Three rings require larger dimensions of the applicator, meaning more energy is lost on the way to the tumour [46]. Based on this study and the dimensions of the head applicator, two rings of 8 antennas will be used. This will allow enough distance between the antennas to avoid cross-coupling while still optimising the available space.

To accommodate for the head support, there will be no antennas at the back of the applicator. This is further supported by the risk of nerve damage that can be brought on by overheating the spinal cord. The antennas were placed evenly over the remaining parts of the applicator to allow for an effective focus for any tumour position. This choice of placement will be examined more in the discussion (section 5.5). The antennas will be placed as shown in figure 34.

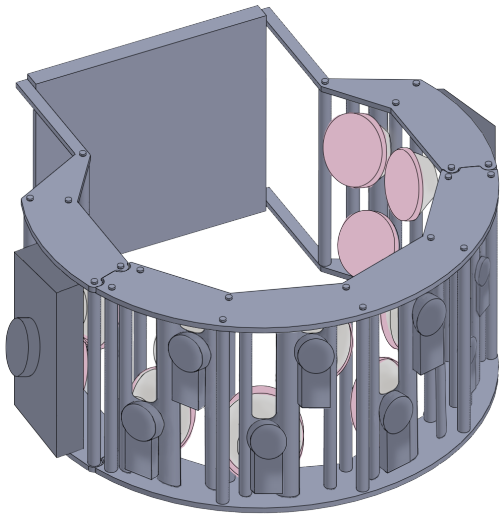

Figure 34: The antenna placement of the hyperthermia applicator. There are no antennas where the head support is placed. There are two rings of 8 antennas. The items behind the antennas are motors for moving the antennas closer to or further away from the patient.

4.3 Cooling Tubes and EM Wires

As there are many parts in need of external resources, such as radiating power and cooling water, there are many tubes and wires coming to and from the applicator. To increase the usability, these are collected and exit the applicator through the back, around the head support.

The full treatment setup, with a patient, can be seen in figure 35.

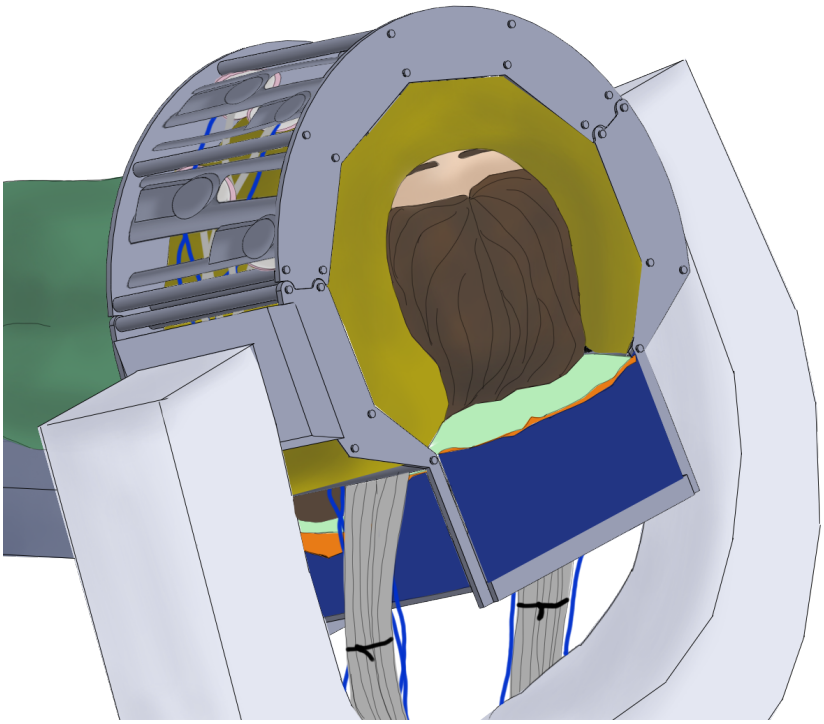

Figure 35: The full setup of the head applicator for hyperthermia treatment. The patient is lying on a gurney with the head applicator on. The patient's head is resting on an immobilising vacuum bag and a waterbag bolus surrounds the patients head, leaving enough room to breath through both the nose and mouth. The applicator has a total of 16 antennas. Holding up the applicator is the positioning machine.

5 Discussion

Developing a hyperthermia treatment system is a complex task, involving many parts. When it comes to deep H&N tumours, the systems required to target them face much higher demands regarding focusing ability compared to other systems. The many types of critical tissue in the region, the depth of the target and the geometry of the head provide challenging obstacles to overcome. The antennas, bolus and antenna applicator make up the main parts of the system. The two latter have been designed for the head applicator within this project and will be discussed in this section.

5.1 Comparison of Hydrogel, Hydrogel with Cooling and Waterbag

Based on the results of the experimental bolus evaluation without a MW antenna, the difference in effect between the hydrogel with an active cooling system and without one was insignificant. Both systems had a rapid increase in temperature in the beginning, which then slowed down as the phantom and hydrogel moved towards the same temperature. The difference that can be observed is a slight incline in the graph for the hydrogel without cooling while the hydrogel with cooling seems to have reached its steady state. The waterbag held the same temperature during full two hours. With the waterbag as a bolus the phantom temperature varied greatly between different parts, but decreased more rapidly than when the hydrogels were used. From this experiment, it can be observed that the waterbag is for temperatures under 25°C more effective at cooling compared to the the hydrogels. At these temperatures, the extra effort required for active cooling of the hydrogel is not worth it. Worth considering is that the hydrogel with cooling had warmer water due to experimental issues. This probably had some effect on the results, but it is unlikely that the increased temperature would make a substantial difference in the hydrogel's cooling ability.
With the addition of a MW antenna to the setup, a drastic change in the comparison between the hydrogel with and without active cooling was observed. The temperature during the experiment with the hydrogel without cooling reached 110°C after only 2000s (30 min), before MW radiation was turned off due to risk of damaging the temperature probes. In the experiment using the hydrogel with cooling, the MW radiation could be active for the full hour as planned. The highest temperature obtained was 97°C. In contrary form the previous set of experiments without an external heat source, the results when using active cooling show a great improvement from the hydrogel without cooling. Looking at the results from when the waterbag bolus was used, a significant difference in temperature can be seen compared to the other boli. The experiment ran for the full hour and the maximum temperature was 75°C. While the cooling tube in the hydrogel had a large impact in effect when the antenna was used, the waterbag is still a signficiantly more effective cooling system.

When using the antenna, it is interesting to know where the highest temperatures occurred. When using the hydrogel without cooling, the highest temperature was in the center of the phantom up until 20 min into the experiment. At this point, the temperature in probe Ia_4 and Ia_8 shot up, reaching >100°C. A 40°C increase occurred in under a minute. This is odd as this increase could not be seen in the remaining probes, and could have been due to a slight movement of the antenna or something in the room. Another reason could have been due to boiling in the bolus since there was a hole found in the hydrogel at the end of the experiment, restricted by the agar mesh. The hot water might have only passed through the points around these two probes. A more constant increase in temperature can be seen in probe Pc_6, that reached a maximum temperature of 103 °C. The sixth Pc-probe is in the upper part of the phantom (the second probe if counted from the top of the phantom). This is a more expected location for the increase to occur: at the top of the phantom, but not all the way at the edge because the bolus cools it. The hydrogel with active cooling did not have the same increase around the antenna. The highest temperature here was in probe Pc_6, at 97°C. The temperature in the offset phantom-probe Po_4 was almost as high at

95°C. It would have been more expected that it had been the offset probe 6, next to Pc_6, but this might simply be due to a slight misalignment between the probes. For the waterbag, the highest temperature reached was in probe Pc_7, closely followed by probe Po_5.

Although it is interesting to analyse where the highest temperature occurred and how this can be altered, the question to answer is which bolus is the most effective at cooling the phantom. The waterbag bolus kept the temperature significantly lower compared to the hydrogel, both with and without active cooling. The fact that the addition of a single cooling tube significantly increased the cooling ability of the hydrogel, is promising for future development of the gel as a bolus.

5.2 Simulation Accuracy

To facilitate the comparison between the simulated and experimental results, they are presented side-by-side in figure 36.

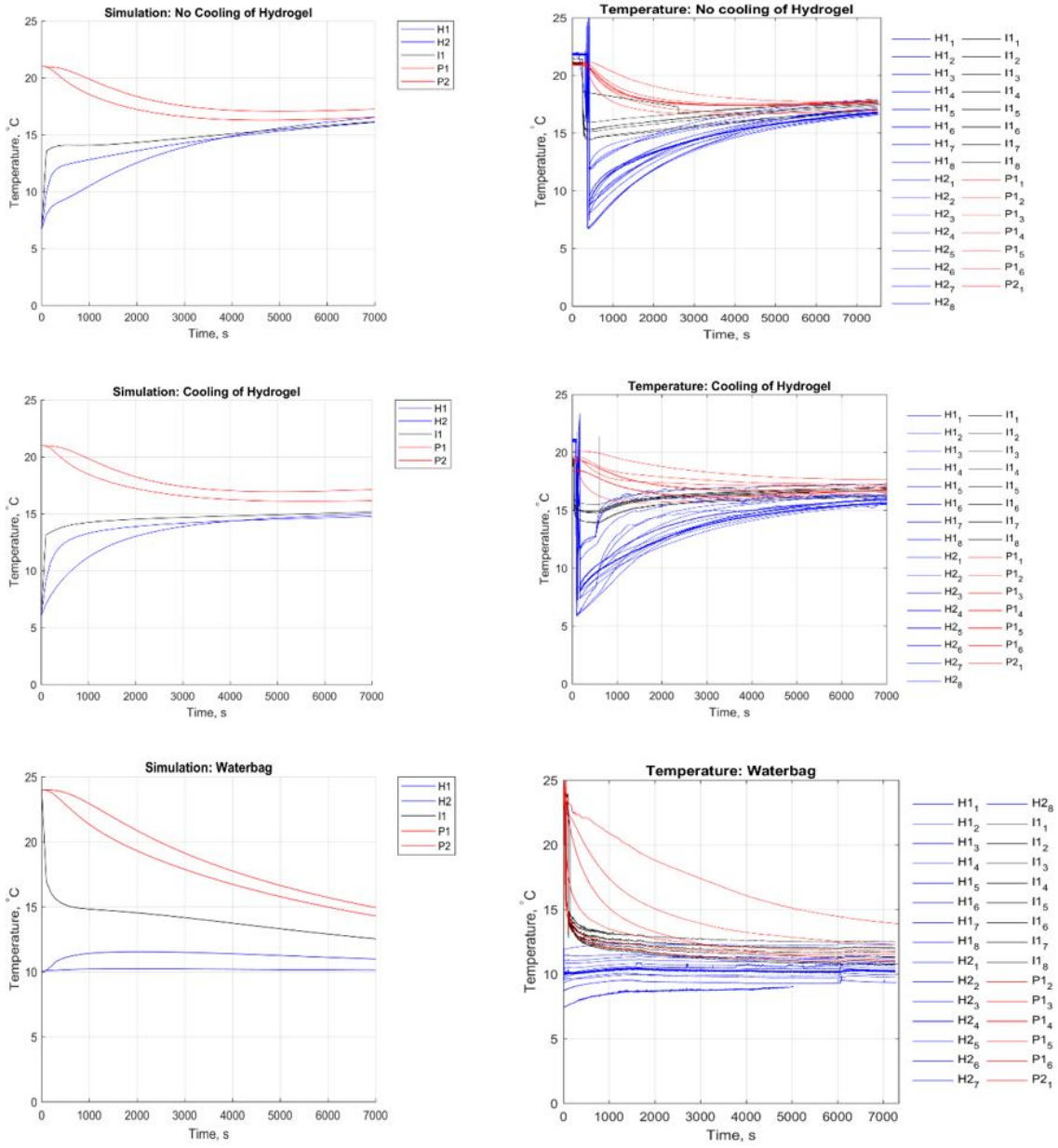

Figure 36: The simulated and experimental results for the bolus evaluation without an external heat source.

Due to the large number of data points in the simulation, determining the exact probe positions was a challenge. There are because of this slight differences in probe placements between simulated probes and experiment probes. Despite this, a clear similarity between simulated and experimental results can be seen. The most substation deviation from its experimental value can be seen in the phantom values, in the waterbag simulation. The flow within the waterbag is more complex than the flow through the hydrogel tube, this could be an explanation for the discrepancy. It could also

have been due to a probe position not matching the real position as well, as mentioned before.

Simulating the results when applying the antenna to the experiments would have been very interesting, but had to be left to another time. Further looking into simulation accuracy is important, especially for hyperthermia applications where the treatment planning is essential for an effective treatment. All in all, the accuracy of the simulations that were obtained showed good results and if more experiments of similar setup was required, they could be done through simulations and accurately predict the outcome.

The most difficult part of doing this analysis was not performing the simulations, but matching the real parameters to the set parameters. In these cases the simulations had to be redone after the physical experiments to make sure that the real temperatures used matched the simulation parameters. Since the simulations had to be recreated, the variations in the experimental setting was a problem. In cases where the simulations are done as an alternative to physical experiments, this in no longer a problem as these parameters can be decided. This can make comparisons within simulations more accurate than in reality where room temperature, humidity etc. are hard to control.

5.3 Choice of Bolus

Kesselring matrices, or as they are also know, decision matrices, are helpful in considering multiple criteria when analysing options. The cooling ability of the bolus is important, but there are also other parameters that matter. The bolus needs to have a good fit to the patient and it is necessary that the are easy for physicians to use during the treatment. Many of today's boli leak easily, causing great discomfort for the patient and takes time and focus away from the treatment. If it breaks or is disfigured when it is placed on a patient, or during the session, the treatment may have to be stopped before it can be fixed.

The strength of the hydrogels is good fit to the patient along with the fact that they do not leak. On the other hand they can be very slippery, making it difficult to place on a patient. They are also slightly deformed during the treatment and will probably have to be melted down and remoulded before the next session. The waterbag bolus is, currently, significantly more effective at cooling and easy to place on a patient. Some of the criteria that the bolus should meet are more important. A weight was set to take this into account. The most important criteria is the cooling, fit and maintenance during treatments. In a clinical setting, the physicians' time is limited and cannot be spent continuously repairing equipment.

Through the use of the Kesselring matrix, all of these criteria and their weights was taken into account. The waterbag still turned out to be the most favourable option, with a rating of 84% of the ideal, compared to 65% and 59% of the hydrogels with and without active cooling respectively.

Since leaking and fit is a challenge with waterbag boli, a second Kesselring matrix was used to evaluate different materials. The fit was determined from the elasticity of the material. Due to a strong unpleasant scent from some of the materials, this was also used as a criteria as it can cause patient discomfort. The most ideal option, the latex spray water bolus has a high elasticity and does not leak. The biggest problems with this bolus is the construction. It is both complex and time-demanding.

5.4 Bolus Design

The bolus design needs to fulfil certain criteria. As discussed extensively, it needs to cool the head and upper neck effectively while keeping a snug fit to the patient's contour. Since the bolus will

cover the head, another criteria is that the patient can breathe. Patients with H&N tumours may experience difficulty breathing through the mouth or nose due to tumour location or swelling. Because of this along with the increased sensitivity of patients undergoing cancer treatment, the bolus was designed to allow breathing through both the nose and the mouth.

Though many design options were considered, most of them aiming to find a way to only have one bolus, in the end it was determined that two boli was the feasible option. The assymetric geometry of a human head and neck was in this case overcome by using a small bolus for the neck and a larger one, with space for breathing. A potential problem with this design is the water flow through the larger bolus. The circulation of water may be hindered in certain regions due to the bottle-neck effect created by the breathing space. Alternative solutions can be adding two more ports in the large bolus, having two circulating systems in it. Another option is extending the bolus above the nose, making the breathing space an oval breathing hole. This may create its own problem, making it harder to breathe with the bolus on. A suitable next step in creating the bolus is performing flow simulations of the suggested model, determining whether or not the flow of issue.

5.5 Antenna Placement

With the exception of the back, the antennas have been evenly distributed around the applicator. The space around the back of the neck is free from antennas, instead making space for a head support and for antenna wires and cooling tubes to exit the applicator. Based on available hyperthermia applicators, this setup is expected to give satisfactory results. There is however always an interest in further improving the setup. Through applying different tumour models and simulating the EM fields of the antennas in all possible positions, the antenna placement beneficial for most types of deep head tumours can be calculated. This type of optimisation is done through the use of algorithms and due to the large amount of data involved, it is a time-demanding process.

5.6 Future Challenges and Continuation Projects

Having worked on such a broad project, involving every part of the applicator, it is easy to get an overview of the hard work that has created the foundation for it as well as the work that needs to be done to further advance it. Potential projects that have already been mentioned includes antenna placement optimisation, developing the cooling system of the hydrogel and improving the waterbag bolus production method in order to make a one-piece bolus. A larger-scale testing of temperature sensation would create a good opportunity to evaluate initial bolus temperatures for deep head tumours. For this purpose, simulations with a patient, bolus and applicator model would be very useful.

Another interesting project would be to look into if it is possible to create a bolus that can be used to cool one area and heat another. This would be very useful for tumour that are both deep and superficial, expanding over different areas. Possible methods of doing this can involve physical barriers or adjusting pressure differences to create flow directions within the bolus.

5.7 Ethical Considerations

Considering the societal aspects, this project has been a part of improving today's methods of treating head and neck tumours. Although the societal benefit can be very positive, it is always required that ethical considerations are taken during the development. Both regarding patients and potential animals that will be part of creating and testing the treatment, but also to those who will use it after it is clinically available. This can involve determining that the treatment does not only equate current treatment methods, but is superior to them. In this case, it has already been

shown in multiple studies that hyperthermia in combination with current methods such as RT and CT has resulted in improved treatment outcome. As this project has not involved any animal or human testing, but rather included computer simulations and tests on phantoms, this has not been of issue. This way of designing projects helps to decrease testing on animals or humans during the development of the treatment method. Of high importance is to recognise that the proposed design is not a finished product and requires further testing to verify that it has the intended effect before it is used for clinical treatments.

It is also always relevant to consider the ecological aspects of a project. The chemicals which were used are edible and commonly added to different food products [47, 48]. Other than everyday-kitchen ingredients such as water and sugar, substances to be used include: LBG, Xanthan Gum and Agar Agar Powder. These are all safe for the environment and can be deposited in the sink. Some of the products used to produce prototypes of different bolus materials were not environmentally friendly. This included the vulcanising glue for the latex, but also the different plastics used. The products were handled according to product descriptions and disposed of properly. The long-term sustainability of the materials used for the project is highly relevant but has to be secondary to their effect, as they will be used for medical purposes and patient well-being has to be prioritised. What was considered during the material evaluation is the durability and maintenance. Products that were more durable and do not require new materials between sessions were prioritised.

6 Conclusion

In this project a head applicator for hyperthermia treatment has been developed and a bolus design has been proposed. The standard solution of a water-filled plastic bag was compared with a novel hydrogel-based bolus. The hydrogel was evaluated with and without an active heating system in form of a silicone tube where water was circulated through. The results showed that the system with most effective cooling was the waterbag bolus. After further analysis of criteria for a good bolus, it was determined that the waterbag bolus was the most favorable option to continue with. The hydrogel had many desirable qualities, such as no leaking and good patient fit, but needs an improved cooling system before it can be applied. The experiments done in the project showed that when an external heat source was used, a microwave antenna, the addition of one cooling tube made a significant different to the cooling ability of the gel. This is promising for its further development. Since the waterbag bolus will be used, different material choices were assessed. The most suitable option was latex spray. The final bolus design suggested for efficient cooling during hyperthermia treatment of head tumours was a waterbag bolus made of latex spray, consisting of a smaller neck piece and a larger head piece to be used simultaneously.

The head applicator frame was then designed. Two large plastic plates, held together by 3D printed pins and screws, will be used. Two layers of antennas are evenly distributed around the applicator, with the exception of the back of the neck. This part has no antennas, making room for a head support and for antenna wires and cooling tubes to exit the applicator.

The overall goal is to get the deep H&N hyperthermia treatment system ready for clinical use. The head applicator developed in this project plays an important role in this, but further testing is required before it can be constructed. The next steps in this development is to finalise the 3D model and perform an optimisation of the antenna positions for head tumours. The bolus design needs to be tested through flow simulations to identify potential problems before construction takes place. When this is done, the applicator can be tested through simulations, whereupon it will be ready for construction. There is, as usual, more work to be done, but the proposed head applicator is a good starting point for what in the close future can be brought to clinical use.

References

[1] P. R. Stauffer and M. M. Paulides, *Hyperthermia Therapy for Cancer*, vol. 10. Elsevier B.V., 2014.

[2] S. Shahsiah, "How is the combination of electric & magnetic waves (electromagnetic wave) illustrated as a single wave?." `https://physics.stackexchange.com/questions/291571/how-is-the-combination-of-electric-magnetic-waves-electromagnetic-wave-illus`, used 2020-01-02, 2016.

[3] P. Takook, M. Persson, and H. D. Trefna, "Performance Evaluation of Hyperthermia Applicators to Heat Deep-Seated Brain Tumors," *IEEE Journal of Electromagnetics, RF and Microwaves in Medicine and Biology*, vol. 2, no. 1, pp. 18–24, 2018.

[4] Federal Communications Commision Office of Engineering and Technology Policy and Rules Division, "FCC Online Table of Frequency Allocations," tech. rep., 2019.

[5] P. och telestyrelsen, "Post- och telestyrelsens allmänna råd (PTSFS 2019:1) om den svenska frekvensplanen," tech. rep., Stockholm, 2019.

[6] N. Vigneswaran and M. D. Williams, "Epidemiologic Trends in Head and Neck Cancer and Aids in Diagnosis," *Oral Maxillofacial Surg Clin N Am*, vol. 26, pp. 123–141, 2014.

[7] J. de Lartigue, "Rising to the therapeutic challenge of head and neck cancer," *Topographic Pathology of Cancer*, vol. 13, no. 2, pp. 73–80, 2015.

[8] V. Grégoire, J. L. Lefebvre, L. Licitra, and E. Felip, "Squamous cell carcinoma of the head and neck: EHNS-ESMO-ESTRO clinical practice guidelines for diagnosis, treatment and follow-up," *Annals of Oncology*, vol. 21, no. SUPPL. 5, pp. 184–186, 2010.

[9] J. Overgaard, "The heat is (still) on - The past and future of hyperthermic radiation oncology," *Radiotherapy and Oncology*, vol. 109, no. 2, pp. 185–187, 2013.

[10] M. M. Paulides, G. M. Verduijn, and N. Van Holthe, "Status quo and directions in deep head and neck hyperthermia," *Radiation Oncology*, vol. 11, no. 21, 2016.

[11] R. Valdagni, M. Amichetti, and G. Pani, "Radical radiation alone versus radical radiation plus microwave hyperthermia for N3 (TNM-UICC) neck nodes: a prospective randomized clinical trial.," *Int J Radiat Oncol biol Phys.*, vol. 15, no. 1, pp. 13–24, 1988.

[12] N. Datta, A. Bose, H. Kapoor, and S. Gupta, "Head and neck cancers: results of thermoradiotherapy versus radiotherapy," *Int J Hyperthermia1*, vol. 6, no. 3, pp. 479–486, 1990.

[13] N. Huilgol, S. Gupta, and C. Sridhar, "Hyperthermia with radiation in the treatment of locally advanced head and neck cancer: a report of randomized trial," *J Cancer Res Ther.*, vol. 6, no. 4, pp. 492–496, 2010.

[14] E. Mandraveli, E. Theodosopoulou, A. Pistofidis, K. Alexandratou, A. Alexandratos, A. Xatzopoulou, D. Boki, and E. Marinos, "The action of hyperthermia in metastatic colorectal cancer in combination with chemotherapy," *Progress in Health Sciences*, vol. 5, no. 1, p. 69, 2015.

[15] H. C. Besse, C. Bos, M. M. Zandvliet, K. van der Wurff-Jacobs, C. T. Moonen, and R. Deckers, "Triggered radiosensitizer delivery using thermosensitive liposomes and hyperthermia improves efficacy of radiotherapy: An in vitro proof of concept study," *PLoS ONE*, vol. 13, no. 9, pp. 1–17, 2018.

[16] P. Gas, "Essential facts on the history of hyperthermia and their connections with electromedicine," *Przeglad Elektrotechniczny*, vol. 87, no. 12 B, pp. 37–40, 2011.

[17] A. Vander Vorst, A. Rosen, and Y. Kotsuka, "6.4 RF AND MICROWAVE ABLATION," in *RF/Microwave Interaction with Biological Tissues*, ch. 6.4, pp. 264–265, Hoboken, New Jersey: John Wiley & Sons, Inc., 2006.

[18] L. Geddes, "d'Arsonval, physician and inventor," *IEEE Engineering in Medicine and Biology Magazine*, vol. 18, no. 4, pp. 118–122, 1999.

[19] G. L. Dewey WC, Hopwood LE, Sapareto SA, "Cellular responses to combinations of hyperthermia and radiation," *Radiology*, vol. 123, no. 4, pp. 463–474, 1977.

[20] N. R. Datta and S. Bodis, "Hyperthermia with radiotherapy reduces tumour alpha/beta: Insights from trials of thermoradiotherapy vs radiotherapy alone," *Radiotherapy and Oncology*, vol. 138, pp. 1–8, 2019.

[21] O. Dahl, "Interaction of Heat and Drugs In Vitro and In Vivo," in *Thermoradiotherapy and Thermochemotherapy*, ch. 5, pp. 103–121, Bergen, Norway: Springer, Berlin, Heidelberg, 1995.

[22] H. H. Kampinga, "Cell biological effects of hyperthermia alone or combined with radiation or drugs: A short introduction to newcomers in the field," *International Journal of Hyperthermia*, vol. 22, no. 3, pp. 191–196, 2006.

[23] M. M. Paulides, J. F. Bakker, M. Linthorst, J. vad der Zee, Z. Rijnen, E. Neufeld, P. M. T. Pattynama, P. P. Jansen, P. C. Levendag, and G. C. Van Rhoon, "The clinical feasibility of deep hyperthermia treatment in the head and neck : new challenges for positioning and temperature measurement," *Physics in medicine and biology*, vol. 55, pp. 2465–2480, 2010.

[24] G. M. Verduijn, P. Togni, Z. Rijnen, and J. A. U. Hardillo, "OC-0335 Feasibility of deep head and neck hyperthermia," in *3rd ESTRO Forum*, (Barcelona, Spain), pp. S165–S166, 2015.

[25] Sensius, "Technology." `https://www.sensius.biz/technology/`, used 2020-01-07, 2016.

[26] P. Takook, M. Persson, J. Gellermann, and H. D. Trefná, "Compact self-grounded Bow-Tie antenna design for an UWB phased-array hyperthermia applicator," *International Journal of Hyperthermia*, vol. 33, no. 4, pp. 387–400, 2017.

[27] H. H. Pennes, "Temperature of skeletal muscle in cerebral hemiplegia and paralysis agitans," *Arch NeurPsych*, vol. 62, no. 3, pp. 269–279, 1949.

[28] G. Barendsen, "Dose fractionation, dose rate and iso-effect relationships for normal tissue responses," *International Journal of Radiation Oncology*, vol. 8, no. 11, pp. 1981–1997, 1982.

[29] A. v. d. K. Michael C. Joiner, "The linear-quadratic approach in clinical practice," in *Basic Clinical Radiobiology*, ch. 9, London: CRC Press, 4th ed., 2009.

[30] C. M. van Leeuwen, A. L. Oei, J. Crezee, A. Bel, N. A. Franken, L. J. Stalpers, and H. P. Kok, "The alfa and beta of tumours: A review of parameters of the linear-quadratic model, derived from clinical radiotherapy studies," *Radiation Oncology*, vol. 13, no. 1, 2018.

[31] Elprocus, "Microwaves – Basics, Applications and Effects." `https://www.elprocus.com/microwaves-basics-applications-effects/`, used 2010-01-02.

[32] M. Visbeck, "Generation of Electromagnetic Waves.." `http://xtide.ldeo.columbia.edu/mpa/Clim-Wat/Climate/lectures/energy/generation.html`, used 2020-01-03, 2003.

[33] Maxwell's Equations.com, "Maxwell's Equations." `http://maxwells-equations.com/`, used 2020-01-07, 2012.

[34] P. J. Bevelacqua, "Bow Tie Antennas." `http://www.antenna-theory.com/antennas/wideband/bowtie.php`, used 2020-01-10, 2009.

[35] Federal Communications Commission, "The FCC's Mission." `https://www.fcc.gov/about/overview`, used 2020-01-10, 2019.

[36] Engineering Toolbox, "Convective Heat Transfer." `https://www.engineeringtoolbox.com/convective-heat-transfer-d{_}430.html`, used 2020-01-03, 2003.

[37] C. Tarawneh, "Heat Transfer Equation Sheet." `https://faculty.utrgv.edu/constantine.tarawneh/HeatTransfer/HeatTransferBooklet.pdf`, used 2020-01-04, 2015.

[38] Byju's Learning App, "Heat Transfer Formula." https://byjus.com/heat-transfer-formula/, used 2020-01-03.

[39] H. D. Trefná and A. Ström, "Hydrogels as a water bolus during hyperthermia treatment," *Physics in Medicine and Biology*, vol. 64, no. 11, 2019.

[40] K. Arunachalam, P. F. Maccarini, J. L. Schlorff, Y. Birkelund, and P. R. Stauffer, "Design of a Water Coupling Bolus with Improved Flow Distribution for Multielement Superficial Hyperthermia Applicators," *Int J Hyperthermia*, vol. 25, no. 7, pp. 554–565, 2010.

[41] B. Elling, *Bringing an H&N microwave hyperthermia applicator from laboratory to clinics*. PhD thesis, Chalmers University of Technology, 2018.

[42] FISO Technolgies, "Fiber Optic Temperature System." https://fiso.com/wp-content/uploads/2018/10/MC-00234-R5-Medical-Temperature-GaAs-sensor-specification-sheet.pdf, used 2020-01-12, 2018.

[43] T. Alhede, M. Eriksson, C. Hjohlman, M. Lord, and V. Petrov, *Temperaturreglering av system för undersökning av blod-hjärnbarriärens kapillärpermeabilitet*. Bachelor thesis, Chalmers University of Technology, 2019.

[44] Blessing Cathay, "Head Supports for Radiation Therapy." https://www.bcc.taipei/RTproducts/product{_}timokit.html, used 2019-12-03.

[45] Meditron, "Vacuum Bag Cushions." https://www.meditron.ch/patient-immobilization/index.php/accessories/cushions/product/56-vacuum-bag-595-x-600-mm-7-liter-\T1\textendash-t-shape-hns, used 2019-12-03.

[46] C. Rigato, *Design of Hyperthermia Applicator for Head and Neck Tumour Treatment : a Simulation Study*. Master's thesis, Chalmers University of Technology, 2013.

[47] DuPont Nutrition & Biosciences, "Grindsted Lbg." https://www.dupontnutritionandbiosciences.com/products/grindsted-lbg.html, used 2019-08-26.

[48] WebMD, "Xanthan Gum." https://www.webmd.com/vitamins/ai/ingredientmono-340/xanthan-gum, used 2019-08-26.

A Appendix A: Recipes

Recipes used to create the hydrogel and the muscle phantom.

Hydrogel Recipe

To make a hydrogel, the following equipment is required.

- Scale
- Hot plate
- Thermometer
- Saucepan or heat resistant beaker
- Electric stirrer or a whisk
- Mould
- Fridge

The ingredients for the hydrogel are:

- Water (tap water was used for this experiment, deionised water should be used for more certain dielectric properties)
- LBG
- Xanthan
- Agar agar powder

Assemble the mould and tape regions where leaks may occur. Calculate the volume of water needed to fill the mould and convert to weight. For X grams water, the mass of the other components is calculated by the formulas below. For the mould used in the project, 2880 g water was needed.

$$\begin{aligned} X \text{ g vatten} &= 2880 \text{ g} \\ X * 0.01 * 0.35 \text{ g LBG} &= 10.08 \text{ g} \\ X * 0.01 * 0.35 \text{ g Xanthan} &= 10.08 \text{ g} \\ X * 0.01 * 0.30 \text{ g Agar} &= 8.64 \text{ g} \end{aligned}$$

Fill the silicone tube with sugar to avoid it collapsing and place it in the mould. To make the hydrogel, start by weighing the saucepan or beaker used. Heat up the water to 60°C. Add LBG while stirring and continue heating to 70°C. Add Xanthan slowly, a little at a time, while stirring, heat until 75°C. Add agar agar powder slowly, a little at a time, while stirring and heat until 90°C.

Remove liquid from the hot plate and weight it. Add water until the weight is the sum of what was originally added (here: 2880 + 10.08 + 10.08 + 8.64 g = 2908.8 g, not including the saucepan). Carefully stir the mix to make sure all the ingredients are equally distributed. Let the hydrogel mix cool until the temperature decreases to 60-70°C. Pour into mould, cover with plastic wrap and put in the fridge until it has solidified. For the amount made in this project, it was left overnight before removal from the mould.

Muscle Phantom Recipe

To make the muscle phantom, the same equipment is required as for the hydrogel. The ingredients needed are:

- Water (tap water was used for this experiment, deionised water should be used for more certain dielectric properties)
- Granulated sugar
- Natrium Chloride (make sure to get salt without iodine)
- Agar agar powder

Before starting, make sure to tape the mould where it might leak. The viscosity of the phantom is lower, meaning it will leak easier! For approximately 2880 ml of the muscle phantom, the following recipe was used.

1347 g water
1093 g sugar
28 g salt
43 g agar

First, make sure to weight the saucepan or beaker used. Heat water, salt and sugar and stir until it is mixed well. At around 60°C, slowly add the agar while continuously stirring. Continue heating until the temperature reaches 90°C. Weigh the mix, adding water until the original weight is reached (here: 1347 + 1093 + 28 + 43 = 2511 g, not including the weight of the saucepan). Mix well and let it cool to 60-70°C. Pour into mould and cover with plastic wrap. Put in the fridge. It was left in the fridge overnight before being taken out of the mould for this project.

B Appendix B: Bolus prototypes

The prototypes made during the project for the evaluation of bolus materials. The latex sheet prototype was made using latex in sheet-form with vulcanising latex glue. The silicone sheet prototype was made using a transparent 0.3mm Essentra part no 81-R1015 (Silex Ltd GP 60 silicone sheet) from Essentra, together with silicone glue. The ports are 3D printed.

Figure 37: The latex (blue) and silicone (white) sheet water boli prototypes made for the material evaluation.

Figure 38: Testing of the prototypes.

C Appendix C: Construction of Spray Latex Bolus

The latex spray bolus was made using a motorised, rotating barrel by Håkan Torén who works closely with the research group. The latex is sprayed, one layer at a time and left to dry between each layer, while the barrel is constantly rotating. After 10 layers, vaseline is rubbed on the part that will become the inside of the bolus, leaving 0.5-1 cm of space at the edges. Then the process is repeated until a double-layered latex bolus has been made. Holes are cut for the ports which can then be used to circulate water through it.